

**WAKE ANALYSIS OF SHIP MODELS TWIN-SCREW MILITARY TYPES**

by

**H. M. Cheng**

and

**J. B. Hadler**

**December 1964**

**Report 1928**

## TABLE OF CONTENTS

ABSTRACT

ADMINISTRATIVE INFORMATION

INTRODUCTION

TEST PROCEDURE AND DATA REDUCTION

PRESENTATION OF DATA

CONCLUSIONS

RECOMMENDATIONS

ACKNOWLEDGMENTS

REFERENCES

## LIST OF FIGURES

Figure 1 - Lines of Twin-Screw Military Ships of DD, DL, DLG and PF Types

Figure 2 - Comparison of Shaft Supports of DD Type

Figure 3 - Coordinate System of Velocity Components

Figure 4 - Wake Velocity Diagram and Test Data, Model 3869

Figure 5 - Wake Velocity Diagram and Test Data, Model 3870-1

Figure 6 - Wake Velocity Diagram and Test Data, Model 3878

Figure 7 - Wake Velocity Diagram and Test Data, Model 3884

Figure 8 - Wake Velocity Diagram and Test Data, Model 4048

Figure 9 - Wake Velocity Diagram and Test Data, Model 4051

Figure 10 - Wake Velocity Diagram and Test Data, Model 4569-1

Figure 11 - Wake Velocity Diagram and Test Data, Model 4659

Figure 12 - Wake Velocity Diagram and Test Data, Model 4711-1

Figure 13 - Wake Velocity Diagram and Test Data, Model 4921

Figure 14 - Wake Velocity Diagram and Test Data, Model 4892

- Figure 15 - Circumferential Longitudinal ( $V_x/V$ ) and Tangential ( $V_t/V$ ) Velocity Distributions at Various Test Radii, Model 3869
- Figure 16 - Circumferential Longitudinal ( $V_x/V$ ) and Tangential ( $V_t/V$ ) Velocity Distributions at Various Test Radii, Model 3870-1
- Figure 17 - Circumferential Longitudinal ( $V_x/V$ ) and Tangential ( $V_t/V$ ) Velocity Distributions at Various Test Radii, Model 3878
- Figure 18 - Circumferential Longitudinal ( $V_x/V$ ) and Tangential ( $V_t/V$ ) Velocity Distributions at Various Test Radii, Model 3884
- Figure 19 - Circumferential Longitudinal ( $V_x/V$ ) and Tangential ( $V_t/V$ ) Velocity Distributions at Various Test Radii, Model 4048
- Figure 20 - Circumferential Longitudinal ( $V_x/V$ ) and Tangential ( $V_t/V$ ) Velocity Distributions at Various Test Radii, Model 4051
- Figure 21 - Circumferential Longitudinal ( $V_x/V$ ) and Tangential ( $V_t/V$ ) Velocity Distributions at Various Test Radii, Model 4569-1
- Figure 22 - Circumferential Longitudinal ( $V_x/V$ ) and Tangential ( $V_t/V$ ) Velocity Distributions at Various Test Radii, Model 4659
- Figure 23 - Circumferential Longitudinal ( $V_x/V$ ) and Tangential ( $V_t/V$ ) Velocity Distributions at Various Test Radii, Model 4711-1
- Figure 24 - Circumferential Longitudinal ( $V_x/V$ ) and Tangential ( $V_t/V$ ) Velocity Distributions at Various Test Radii, Model 4921
- Figure 25 - Circumferential Longitudinal ( $V_x/V$ ) and Tangential ( $V_t/V$ ) Velocity Distributions at Various Test Radii, Model 4892
- Figure 26 - Mean Longitudinal Velocity ( $\bar{V}_x/V$ ) and Mean Tangential Velocity ( $\bar{V}_t/V$ )
- Figure 27 - Calculated Volumetric Velocity ( $\bar{V}_v/V$ ) and Volumetric Mean Velocity
- Figure 28 - Amplitudes and Phase Angles of Various Harmonics of Longitudinal ( $\tilde{V}_x/V$ ) Velocity Components, DD Type
- Figure 29 - Amplitude and Phase Angle of Various Harmonics of Tangential ( $\tilde{V}_t/V$ ) Velocity Components, DD Type
- Figure 30 - Amplitude and Phase Angles of Various Harmonics of Longitudinal ( $\tilde{V}_x/V$ ) Velocity Components, DL and DLG Types
- Figure 31 - Amplitude and Phase Angles of Various Harmonics of Tangential ( $\tilde{V}_t/V$ ) Velocity Components, DL and DLG Types

- Figure 32 - Amplitude and Phase Angles of Various Harmonics of Longitudinal  $(\tilde{V}_x/V)$  Velocity Components, CGN and DLGN Types
- Figure 33 - Amplitude and Phase Angles of Various Harmonics of Tangential  $(\tilde{V}_t/V)$  Velocity Components, CGN and DLGN Types
- Figure 34 - Velocity Diagram
- Figure 35 - Mean Advance Angles  $(\bar{\beta})$ , Variations in Beta Angles  $(\Delta\beta)$  And Pressure Factor  $(P)$
- Figure 36 - Variation in Angle of Advance and Frequency of Plus  $\Delta\beta$ , DD Type. (With Struts)
- Figure 37 - Variation in Angle of Advance and Frequency of Plus  $\Delta\beta$ , DD Type (With Skeg or Bossing)
- Figure 38 - Variation in Angle of Advance and Frequency of Plus  $\Delta\beta$ , DL and DLG Types
- Figure 39 - Variation in Angle of Advance and Frequency of Plus  $\Delta\beta$ , CGN and DLGN Types
- Figure 40 - Amplitude of First Harmonic of Tangential Velocity,  $(\tilde{V}_t/V)_1$ , versus Angle of Shaftline to Baseline

## NOTATION

D	Propeller diameter
$J_a$	Apparent advance coefficient $V/nD$
n	Propeller revolutions
P	Pressure factor $(V_b^2)_{\max} / \overline{V_b^2} - 1$
R	Radius of propeller
r	Radial coordinate
U	Blade element velocity
V	Model or ship velocity
$\underline{V}$	Resultant wake velocity vector
$V_b$	Resultant inflow velocity to blade
$\bar{V}_b$	Mean resultant inflow velocity to blade
$V_r$	Radial component of velocity vector
$\bar{V}_r$	Mean radial component of velocity vector
$V_t$	Tangential component of velocity vector
$\bar{V}_t$	Mean tangential component of velocity vector
$(\tilde{V}_t)_n$	$n^{\text{th}}$ harmonic amplitude of tangential velocity
$V_{tr}$	Transverse component of velocity vector
$\bar{V}_v$	Volumetric velocity
$V_x$	Longitudinal component of velocity vector (normal to the plane of propeller)
$\bar{V}_x$	Mean longitudinal component of velocity vector
$(\tilde{V}_x)_n$	$n^{\text{th}}$ harmonic amplitude of longitudinal velocity
X, Y, Z	Cartesian coordinates
$\alpha_h$	Projected angle of velocity vector on X-Y plane
$\alpha_v$	Projected angle of velocity vector on X-Z plane

$\beta$	Advance angle in degrees
$\bar{\beta}$	Mean advance angle
$\Delta\beta$	Variation of advance angle from its mean
$\theta$	Position angle (angular coordinate) in degrees

Hull coefficients are in accordance with SNAME-recommended standard.

## ABSTRACT

This report, the second of a series on studies of the wake in the propeller plane of ship models, presents the results of analysis of the wake of twin-screw, military-type ship models using the IBM-7090 computer. The data presented are the interpolated longitudinal and tangential velocity distributions, their computed mean values, the harmonic contents of these velocity components, the maximum variations in the resultant inflow velocity, and the advance angles and their variations. Also included are the calculated volumetric wake velocities.

## ADMINISTRATIVE INFORMATION

The work reported herein was sponsored by the Bureau of Ships as part of the General Hydrodynamics Research Program.

## INTRODUCTION

The problems of propeller cavitation, noise and vibration have long been matters of great concern to naval architects. During the past decades, the trend of most ship design has been toward high speed and, therefore, high power ships. As this trend continues, the seriousness of these problems is magnified, and in many instances, they become the primary design considerations, especially for some of the modern naval ships. The source of the problems is attributed, at least partially, to the non-uniform character of the velocity field in which a propeller operates. In order to minimize the serious effect of these phenomena on the life of

machinery and equipment, and on the performance and the safety of ships, it is essential to know more about the flow pattern behind a ship and its characteristics, and to find means to reduce these problems to an acceptable degree.

Because of the complexity of the ship configuration, there is no theoretical means by which wake behind a ship can be adequately estimated; consequently, naval architects have relied upon experimental methods from which velocities at discrete test points are obtained. In the past, these experimental data could be analyzed only to a limited extent using time-consuming hand computation and curve-fairing techniques. These analyses usually provide information on the magnitude and direction of the velocity at the test points, and a map of isovelocity contours.

The advent of the digital computer has revolutionized our concepts and procedures of numerical computation, and has made it possible to obtain additional useful information from a more detailed analysis of the experimental data. The first such attempt was made on the wake analysis study conducted on the SSB(N)598-Class submarines.<sup>1</sup> This also opened the possibility that much unassimilated information existed in the numerous three-dimensional wake surveys conducted at the Taylor Model Basin during the past 20 years. These data had originally been analyzed individually for the particular ship design involved. By viewing them as a whole, it was hoped that guidance would be provided to the naval architects and marine engineers on the wake characteristics of the various types of hull forms built during the past two decades. With this goal in mind, a research project was initiated by the authors to reanalyze all of the three-dimensional wake surveys conducted at the Model Basin.

---

<sup>1</sup>References are listed on page 16. 2



For convenience, the ship models in this project have been grouped into two major categories, naval and merchant types. Each type has been further subdivided into smaller groups by numbers of propellers, i.e., single screw, twin screw, and quadruple screw. Separate reports on the studies of each group will be issued.

The first report<sup>2</sup> presented the results of the analysis of the wake of single-screw, DE-type models. This second report presents the results of the wake analysis of twin-screw, military-type ship models. This group includes 11 models which are broken into the following groupings: 4 DD's, 3 DL and DLG's, 3 CGN and DLG(N)'s,<sup>6</sup> and a twin-screw patrol escort, PF.<sup>5</sup> All of these ship models have stern hull configurations which are quite similar. Models 4921 and 4892 have the widest deviation from the group; Model 4921 has a large bow dome and Model 4892 has hull proportions which differ rather markedly from the norm of the group and a propeller location which is relatively closer to the hull. Model 4892 has been included in this report for comparison purposes.

Figure 1 shows sketches of the hull lines of one model from each group, and Table 1 provides the model data and the major hull coefficients. All the models except those representing the destroyer type were equipped with twin-arm struts to support the outboard portions of the shaft. The four destroyer models provide an interesting comparative study. Models 3869 and 3884 are the same except that Model 3869 is slightly longer (an additional 0.76 feet of parallel middle body) and has a twin-arm intermediate strut whereas Model 3884 has a single-arm intermediate strut.

Model 3870-1 is similar to 3869 except that the shaft is enclosed in a skeg. Model 3878 is provided with a partial bossing with the aftermost portion of the shaft supported by a twin-arm strut. Figure 2 provides a pictorial comparison of these sterns.

The data reported are the axial and tangential wake velocity distributions in the plane of a propeller, their computed circumferential mean values and harmonic contents at various radii, the maximum variations in the resultant inflow velocity, and the advance angles and their variations. The calculated volumetric wake velocities are also presented. The reader is referred to Reference 2 for discussions of the test procedures, the method of data reduction, and the applications of wake data in propeller-ship design.

#### TEST PROCEDURE AND DATA REDUCTION

The wake surveys for the various models contained in this report were conducted in the deep-water towing tanks at the Model Basin. The time period within which the surveys were made spans approximately 20 years and dates back to the time when the DD-692-Class destroyers were being developed during the latter years of World War II.

To obtain the velocity field behind a ship model, the pressures at various points in the field are measured with a spherical pitot tube while the model is being towed at a given speed and draft condition. The dynamic pressure at test points are then derived from the measured pressures.

Only the field of the port propeller is surveyed for the ships reported here because for a twin-screw ship, the flow at the propeller plane is assumed to be symmetrical with respect to the center vertical

axis of the ship. On most ships, the port propeller shaft has a larger shaft angle dictated by the machinery arrangement. When the tests were conducted, all appendages except the rudder were installed. Measurements were made at only one speed for each of the models. It should be noted in Table 1 that the speeds within each group were comparable.

The field points (see Figure 3), in general, were suitably selected in the plane of the propeller circumferentially distributed along several radii. Since the surveys were conducted at various times, under different circumstances, and for varying purposes, the lack of uniformity in these tests is to be expected. The selection of field points is no exception. For the surveys reported, the total number of field points surveyed ranged from 30 at three radii to 64 at four radii for one of the latest models, 4921. The angular intervals also vary, and the points are usually not equally spaced for each survey.

The pitot tubes used for the surveys were either of the so-called 5-hole design or of the 13-hole design. The tubes have two rows of radial holes, one row in each of the vertical and horizontal planes with a common center hole. The 5-hole tube has three holes in each row, and the 13-hole tube has seven. The construction and calibration, as well as the test and data analyzing procedures of the 5-hole tube, are described in References 3 and 4. The 13-hole tube has a similar construction. For each test point, 13 readings are taken; the magnitude of the resultant velocity vector  $\underline{V}$ , its projected angles ( $\alpha_v$  and  $\alpha_h$ ) on the vertical and horizontal planes, and thus its direction are obtained by desk computation and curve-fairing techniques. The 13-hole pitot tube was used for the measurements on the four World War II destroyers; the 5-hole tube was used for the remainder of the models.

Reference 2 describes in detail the method of mounting and aligning the pitot tube equipment on the model to obtain the desired field points. It has been the practice since 1954 to mount the pitot tube axis parallel to the propeller shaft axis. Prior to that date, the pitot tube axis was mounted parallel to the baseline and the wake survey made in the vertical plane through the center of the propeller on the shaft axis. In this report, the four wake surveys made on the DD-692-Class destroyers were made in the latter manner. Thus, it has been necessary to correct these data for the slope of the shaft which was 4.3 degrees. The velocity diagrams in this report are different by the amount of the shaft slope from those previously published by the Model Basin.

The test data are used as input to the computer program for analyses. The procedure of data reduction is similar to that described in Reference 2.

#### PRESENTATION OF DATA

Two types of information are presented: the test data and the computed results. The test data are those obtained from the model experiments at the discrete test points. The computed data are the quantities calculated on the basis of the test data. For convenience, a standard length on waterline of 400 feet and a standard propeller diameter of 12 feet were chosen for the presentation of the computed results.

The test data are tabulated in Figures 4 through 14. Also shown are the transverse velocity vectors in the plane of the propeller at the various test points. The body plan in the proximity of the propeller plane and the propeller shaft struts are also given in these figures.

Figures 15 through 25 show the interpolated circumferential distribution of the longitudinal and tangential velocity components at the

test radii for the various ships. The nondimensionalized radii are those of the model propeller designed for the ship. Where the faired curves do not pass through the test data points, the data are considered in question. In this series of tests, measurements behind the struts have been noted to be erratic. It has been shown in Reference 2 that the effect of struts is relatively small; thus in analyzing the data, the faired values are used.

From Figures 15 through 25, it may be observed that the velocity patterns at the various radii tested have a characteristics shape. The longitudinal velocity component shows a velocity defect in the region nearest the hull and in the shadow of the propeller shaft. The tangential velocity component shows a nearly sinusoidal distribution curve resulting from the angularity of the flow into the plane of the propeller. The angle of shaftline to the baseline and the angle the shaftline makes with the intersecting line on the hull of a plane which is normal to the hull and passes through the shaft centerline are given in Table 1 for comparison purposes. It can be noted that the variation in magnitude of these values is quite small for the models contained in this report, yet the variations in the tangential component  $V_t/V$  is greater than would be indicated by the variation in these two angular quantities. This will be discussed in greater detail in a later section.

The results of the tests on the DD-692-Class destroyers provide some interesting comparisons. The longitudinal velocity defect for the forms with the skeg and with the large bossing and strut (Figures 16 and 17) is somewhat more severe than with struts (Figures 15 and 18). The tangential velocity also shows a steeper velocity gradient in the region behind the skeg or bossing.

Models 3884 and 3869 also provide information on the comparative accuracy of measurements. The only difference in these two models is that Model 4869 is 0.76 feet longer and has a twin-arm intermediate strut whereas Model 3884 has a single-arm intermediate strut. As shown in Reference 2, these differences are found to have negligible effect upon the wake patterns, yet it may be noted that the longitudinal velocity defects for these two models are somewhat different. This is believed due to the instability of the flows in that region and the relatively small number of data points.

The DL and DLG types (Figures 19 through 21) show a very small longitudinal velocity defect in a relatively small arc in the shadow of the shaft. On the other hand, the DLG(N) and CG(N) models (Figures 22 through 24) show considerably more defect and over a considerably wider arc of the circle. Finally, the patrol escort (Figure 25) shows not only the influence of the shadow of the shaft but also the influence of the hull and its boundary layer. It may be noted (from Figures 4 through 14) that the amount of propeller within the block of the hull, i.e., the portion of the propeller that is above the baseline, for each of these groups of ships is progressively increased.

The circumferential distribution curves of the longitudinal and tangential velocity components are analyzed for their harmonic contents. The circumferential mean values obtained at various radii are shown in Figure 26. The mean longitudinal velocity distribution for various ships spread within a band from 0.95 to 1.05. However, for each type, there is fairly good agreement among the various models so that separate curves may be drawn to represent the typical radial distributions of mean longi-

tudinal velocity for the various types of ships analyzed here. The mean values of the tangential velocity components are within the narrow band of  $\pm 0.02$ . For all practical purposes, they can be considered to be zero.

Figure 27 shows the calculated volumetric velocity and its mean value for various ships; their definitions are given in Reference 2.

The amplitude and the phase angle at various orders of harmonics are obtained from the harmonic analysis of the velocity curves. Figures 28 through 33 show the amplitudes and phase angles for the harmonics of orders up to 7. The spots shown in these figures are the calculated values of the amplitudes and the phase angles at the test radii for the various models included. They exhibit quite a large scatter among the models, indicating that the harmonic contents of the circumferential distributions of the wake velocity are somewhat different even though the mean values are fairly close.

In general, these curves, both longitudinal and tangential, show that there is a monotonic decrease in amplitude with increasing order of harmonic. The values are nearly always less than 1 percent of the free stream velocity above the fourth harmonic. The amplitudes also tend to show less scatter with increasing order of harmonic. On the other hand, the phase angle tends to show increasing scatter with increasing order of harmonic. This is to be expected and is attributable to a number of causes, namely, the lack of sufficient measurements in the shadow of the shaft and the increasing uncertainty of the measurements themselves in this region due to instability of the flow around the shaft.

In order to present a clearer picture and to avoid cluttering the figures with curves, lines were drawn for the representative models only,

that is, Models 3870-1 and 3884 for the DD's, Model 4048 for the DL and DLG's, and Model 4921 for the CG(N) and DLG(N)'s. The curves on Figures 28 and 29, the group of destroyers, are particularly revealing. It may be noted that the dashed curves which represent the two models equipped with skegs and/or bossing show greater amplitude values than the solid curves which represent the destroyers with struts. This shows rather clearly that if unsteady propeller forces generated from the spacial wake variation are important, strut supports are markedly superior to skegs or bossings.

For the purpose of furnishing useful information in analyzing the performance and the cavitation characteristics of a propeller operating in a nonuniform wake field, the wake data are further analyzed in terms of maximum variations, or maximum fluctuations in the resultant inflow velocities to the propeller blade and in the advance angles.

As shown in Figure 34, the velocity at the blade element depends on the propeller rotational speed. In order to establish proper geometric relationships, it is necessary to assume certain operating conditions, namely, the advance coefficient  $J_a$ . Since the designed advance coefficient for the various models varies from 0.768 to 1.049, an advance coefficient of 0.85 was arbitrarily chosen for this analysis. As shown in Reference 2, the computed quantities show a relatively small change over a wide range of  $J_a$  values.

Figure 35 shows the calculated mean values of the advance angle  $\bar{\beta}$  at various radii and their maximum variations  $\pm \Delta\beta$ . For clarity, curves are drawn to represent each of the types. This means that the advance angle may be anywhere within the band bonded by  $\bar{\beta} + (+\Delta\beta)$  and  $\bar{\beta} + (-\Delta\beta)$



curves in a quasi-steady sense. It may be noted that the mean advance angles for all the models agree fairly well. They all fall within a band of less than .2 degrees. But the maximum variations of advance angles are widely scattered, especially the negative variation  $-\Delta\beta$ .

The primary factor in determining the magnitude of  $-\Delta\beta$  quantity is the longitudinal velocity defect in the region of the propeller shaft shadow. As previously discussed, these values are not very precisely determined largely due to the limited number of measurements and the instability of the flow crossing the propeller shaft. Despite this limitation, significant comparisons can still be made.

A comparison of the DD's equipped with struts (Models 3869 and 3884) to those equipped with skegs and bossings (Model 3878-1 and 3878) shows the clear superiority of the struts in reducing the tendency towards cavitation, particularly back cavitation.

Also shown on the same figure are the so-called pressure factors which represent the minimum pressure at the propeller blade element resulting from the fluctuations in the inflow velocity expressed as per cent of the mean resultant velocity at that particular blade element. This quantity is affected primarily by the variations in the tangential component of wake velocity, and consequently, the group of DL and DLG's, which has a larger variation in tangential velocity, has a larger fluctuation in the resultant inflow velocity.

The  $\pm \Delta\beta$  values shown in Figure 35 represent the maximum variations from the mean. They show the maximum (or minimum) magnitude of the angle of advance but give no indication of the variation within one propeller revolution. The question may then arise as to what percent of time (or

how much of an arc) the blade element will be subjected to this maximum fluctuation as the propeller rotates. The analysis has been extended in this report to include this information. The results are shown in Figures 36 through 39. In these figures, three sets of curves are shown in regard to the variations of the angle of advance; they are marked 100, 80, and 60 percent. The curves marked 100 percent are those shown in Figure 35. The curves marked 80 percent mean that 80 percent of the time the values of the  $\beta$  angle are within the bounds of  $\bar{\beta} + (+\Delta\beta)_{80}$  and  $\bar{\beta} + (-\Delta\beta)_{80}$ . The curves marked 60 percent have a similar meaning.

It should be observed that the difference for the positive  $\beta$  values between these three curves is small relative to those for the negative  $\Delta\beta$  values. This indicates that for the most part, the circumferential longitudinal velocity distributions curve is rather flat except in the shaft shadow where the velocity defect occurs, resulting in a relatively large  $-\Delta\beta$  values.

Also shown on these figures are the curves showing the frequency of  $+\Delta\beta$ , i.e., the percent of time (or percent of circumference) in which the values are positive. The fact that these curves are approximately 50 percent indicates that for the model analyzed here, the dominant influence comes from the tangential velocity component.

As has been shown in the preceding paragraphs, the tangential velocity component is quite important to the cavitation problem as it contributes to some of the fluctuations in the advance angle and is the dominant influence in the fluctuation of the inflow velocity to the propeller blade elements. Since the tangential velocity is characteristically

sinesoidal, the first harmonic is the dominant term. The amplitudes of this first harmonic may then be used to represent closely the tangential flow at the propeller plane due to both the angularity of the shaft and the influence of the hull. The angles which the shaftlines make with the baseline for the various models reported here vary, ranging from 2.5 to 5.5 degrees; they are tabulated in Table 1. In order to show the effect of the shaft angularity and the effect of the hull on the tangential velocity, the amplitudes of the first harmonic of the tangential velocity components for these models at  $r/R = 0.5, 0.7, \text{ and } 0.9$  are plotted against the shaftline-baseline angles in Figure 40. This plot shows that the ships tend to fall into the groupings already established and that the CGN and DLGN group tends to have the smallest tangential flow, whereas the DL's tend to have the greatest. To date, the authors have not been able to find any means of correlating this angularity of flow to any of the geometric characteristics of the hull.

#### CONCLUSIONS

1. Even though the bow lines of the various types of models studied are quite different from each other, their stern configurations are somewhat similar. Inasmuch as the data for all the models show a similar wake pattern, it may be concluded that the variation in the design of the forebody has very little effect on the stern wake. This is further demonstrated by the comparison of Model 4892, a patrol ship, with other models of destroyer and cruiser-type ships. This conclusion was also drawn in Reference 2.

2. In view of the fairly good agreement of data between the various groups of models of similar stern configuration, we may expect

a similar wake pattern for models with a stern configuration similar to the ones studied here. The circumferential mean nondimensional longitudinal velocities at 0.7 radius are 1.015 for DD's with struts, 0.980 for DD's with skegs or bossings, 1.025 for DL and DLG's, and 0.950 for CGN and CLGN's. They are linearly distributed along the radius at an approximate rate of -0.05 per 0.1 of radius. For all practical purposes, the circumferential mean tangential velocity is zero.

3. It has been shown that the amplitudes and phase angles of the various harmonics of the circumferential longitudinal and tangential velocity distribution curves vary among the various models even though for each group the mean values of these velocity components are quite close. This points up the fact that the harmonic contents of the circumferential velocity distributions are sensitive to the actual fluctuations. Any future experimental work should be concentrated upon more carefully delineating the velocity pattern in the shadow of the propeller shaft. This would permit accurate determination of the magnitudes of the propeller blade frequency and of the higher harmonics.

4. The harmonic analysis of the longitudinal and tangential velocity components shows a monotonic decrease in amplitude with increasing order of harmonic. The single amplitude values are less than 1 percent of the free-stream value above the fourth harmonic. This would indicate if unsteady propeller forces are important, the higher the number of blades, the lower the forces on the propeller shaft, whether axial, transverse, or vertical.

5. The positive and negative variations in the advance angles from the mean are not too consistent among the models within the various groups, but they do show a trend. It may be expected that propellers operating in such wakes most probably will experience a large change of angle of attack in the narrow region of propeller shaft shadow, and especially near the hub. The maximum fluctuation in the resultant inflow velocity in terms of the mean values are in the order of 25 percent at the hub and diminish to 9 percent near the tip for the DL and DLG's. For the CGN and DLGN's and for the DD's, the fluctuations are approximately 25 and 5 percent lower than those of the DL's, respectively.

6. Comparisons of strut with skeg or bossing supported propeller shafts shows that struts are markedly superior so far as cavitation and the unsteady propeller forces are concerned.

#### RECOMMENDATIONS

As a result of this analysis, the following recommendations are made regarding future work on the twin-screw, destroyer-cruiser type of ships.

1. Any future wake surveys conducted on ship models of these types should include a more careful exploration of the region behind the propeller shaft.

2. The data presented in this report may be used directly for preliminary propeller design purposes on future designs of ships with hull characteristics, design speeds, and, above all, stern configurations similar to those contained in this report.

3. The effect of the ship wave train at different speeds upon the wake pattern is not known and may be important. This effect should be examined by testing a model at different speeds or by testing a mirror model.

#### ACKNOWLEDGMENTS

The authors wish to express their thanks to the personnel of Max H. Morris, Inc., for assistance in the collection of data and in the preparation of final graphs, and to Mr. George Smith of the Applied Mathematics Laboratory for his help in the computer work.

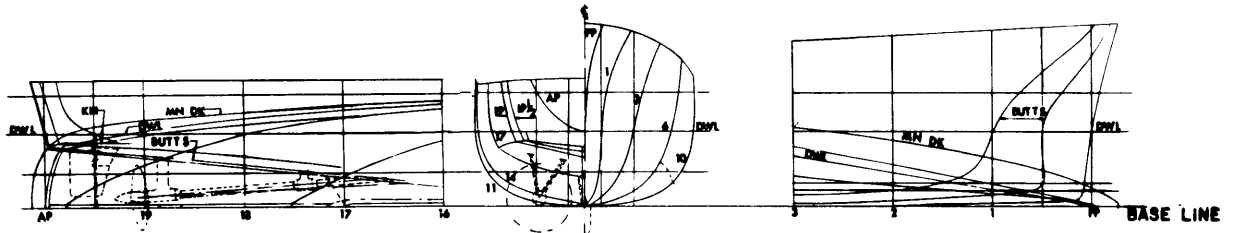
#### REFERENCES

1. Hadler, J.B., and Wermter, R., "Comparison of Wake Parameters of Various Modified Hull Forms of SSB(N)598-Class Submarine," David Taylor Model Basin (DTMB) Report C-1390 (Jun 1962) CONFIDENTIAL.
2. Cheng, H.M., and Hadler, J.B., "Wake Analysis of Ship Models, Single-Screw DE-Type," DTMB Report 1849 (Jun 1964).
3. Pien, P.C., "Five-Hole Spherical Pitot Tube," DTMB Report 1229 (May 1958)
4. Stuntz, G.R. et al., "Series 60 - The Effect of Variation in Afterbody Shape Upon Resistance, Power, Wake Distribution, and Propeller-Excited Vibratory Forces," Transactions of The Society of Naval Architects and Marine Engineers, Vol. 69 (1961).
5. West, E.E., "Powering Predictions for a Patrol Escort Represented by Model 4892," DTMB Report C-1360 (Oct 1961) CONFIDENTIAL.
6. West, E.E., and Hankley, D.W., "Powering Characteristics, Velocity Survey in Way of Propeller and Appendage Orientation Data for a Guided-Missile Frigate DLG(N)35, Model 4921," DTMB Report C-1499 (Nov 1962) CONFIDENTIAL.

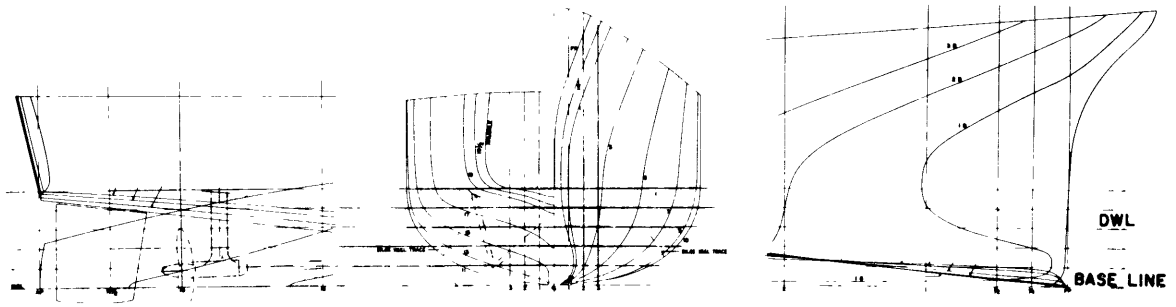
TABLE 1  
Model Data

Particulars:	Model 3869	Model 3870-1	Model 3878	Model 3884	Model 4048	Model 4051	Model 4569-1	Model 4659	Model 4711-1	Model 4921	Model 4892
Length of LWL, $L_{WL}$ Ft	20.76	20.76	20.76	20.00	20.00	20.00	20.47	26.47	22.44	22.51	22.57
Beam, B Ft	2.197	2.197	2.197	2.197	2.070	2.010	2.085	2.718	2.363	2.369	2.856
Draft, H Ft	0.705	0.705	0.705	0.711	0.690	0.588	0.661	0.823	0.769	0.844	0.799
Displacement, FW Ton	0.474	0.474	0.474	0.448	0.368	0.323	0.340	0.767	0.586	0.635	0.636
Test Velocity, V Kn	6.99	6.99	6.99	6.99	6.57	7.48	7.15	5.87	6.21	5.91	5.89
$V/\sqrt{L_{WL}}$	1.50	1.50	1.50	1.56	1.47	1.68	1.58	1.14	1.31	1.25	1.24
Propeller Diameter, D Ft	0.673	0.673	0.673	0.665	0.588	0.585	0.585	0.650	0.623	0.520	0.520
Advance Coeff., $J_a = V/nD$	0.824	0.847	0.834	0.801	1.049	0.856	0.857	0.927	0.867	0.881	0.768
LWL Coefficients:											
$C_B$	0.531	0.531	0.531	0.515	0.461	0.489	0.436	0.466	0.510	0.507	0.444
$C_P$	0.636	0.636	0.636	0.619	0.574	0.611	0.564	0.577	0.620	0.627	0.610
$C_X$	0.835	0.835	0.835	0.832	0.805	0.801	0.773	0.807	0.820	0.818	0.728
$C_{PA}$	0.677				0.594	0.653	0.594	0.616	0.640	0.640	0.689
$C_{PVA}$	0.636				0.568	0.594	0.536	0.574	0.630	0.580	0.621
$L_R/L_{WL}$	0.434	0.434	0.434	0.450	0.478	0.453	0.460	0.469	0.450	0.480	0.436
$L_{WL}/B$	9.45	9.45	9.45	9.10	9.66	9.93	10.00	9.74	9.50	9.50	7.90
B/H	3.11	3.11	3.11	3.10	3.00	3.42	3.10	3.30	3.07	2.81	3.56
$\Delta_{SW}/(0.01 L_{WL})^3$	54.52	54.52	54.52	57.53	47.13	41.51	40.81	42.51	53.50	57.25	56.91
Appendages:											
Bow Dome	none	none	none	none	none	none	none	none	none	yes	none
Shaft Support	struts	skeg	bossing	struts	struts	struts	struts	struts	struts	struts	struts
Intermediate Struts	2-arm	--	2-arm	1-arm	2-arm	2-arm	2-arm	2-arm	2-arm	2-arm	2-arm
Angle - Port Shaft with $\bar{E}$	4.3°	4.3°	4.3°	4.3°	3.5°	5.5°	4.5°	3.0°	4.0°	4.1°	2.5°
Angle - Port Shaft with Hull	9.2°	9.2°	9.2°	9.2°	8.7°	9.5°	13.0°	7.3°	8.5°	13.2°	13.0°

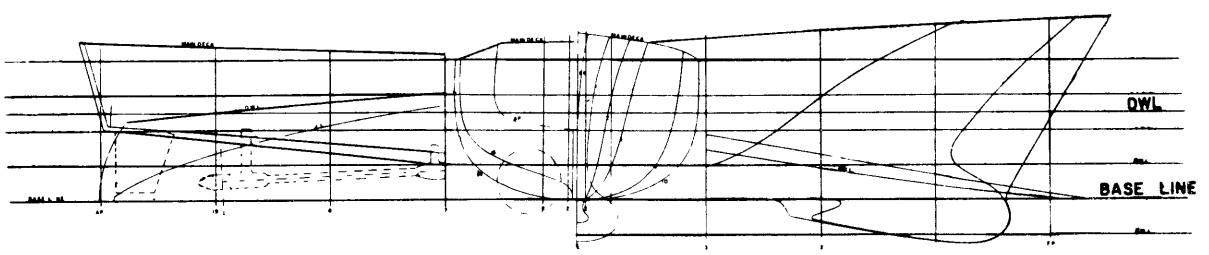
Note: Escort and Destroyer Models 3675A, 3740, 3757 and 3800 are not included in this report because of either inadequate or inaccurate data.



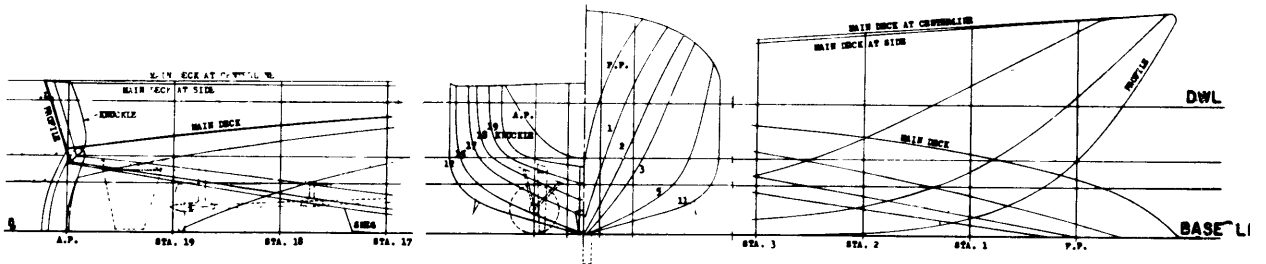
MODEL 3869 (DD)



MODEL 4048 (DL)



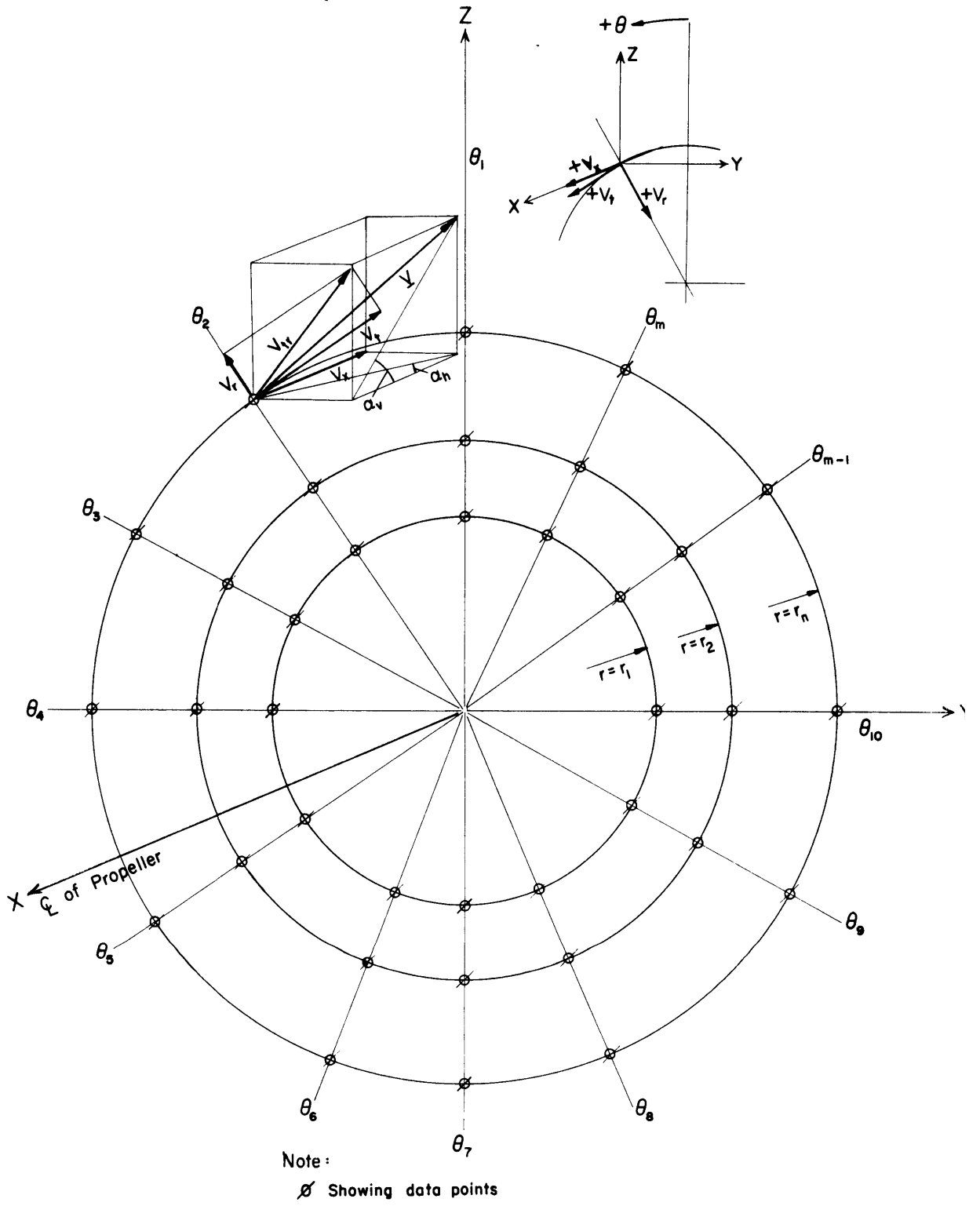
MODEL 4921 (DLGN)



MODEL 4892 (PF)

Figure 1 - Lines of Twin-Screw Military Ships of DD, DL, DLG, and PF Types





Looking Forward

Figure 3 - Coordinate System of Velocity Components

VELOCITY SURVEY IN WAY OF THE PROPELLER	
TWIN SCREW SHIPS	
MILITARY TYPE	
MODEL 3869	
MODEL DIMENSIONS	
LENGTH (LWL)	20.759 FT
BEAM	2.196 FT
DRAFT	.705 FT
DISPLACEMENT	.474 TONS F.W.
PROPELLER DIAMETER	.673 FT
SPEED	7.00 KT
TEST 0	
SEPTEMBER 1944	

- $r/R$  IS THE DISTANCE FROM THE PROPELLER AXIS ( $r$ ) EXPRESSED AS A RATIO OF THE PROPELLER RADIUS ( $R$ ).
- $\theta$  IS THE ANGLE MEASURED FROM THE TOP OF THE PROPELLER DISK IN A COUNTERCLOCKWISE DIRECTION.
- $V$  IS THE SHIP SPEED.
- $V_x$  IS THE LONGITUDINAL (NORMAL TO THE PLANE OF SURVEY) COMPONENT OF THE WATER VELOCITY AND IS POSITIVE IN THE ASTERN DIRECTION.
- $V_t$  IS THE TANGENTIAL COMPONENT OF THE WATER VELOCITY AND IS POSITIVE IN THE COUNTERCLOCKWISE DIRECTION.
- $V_r$  IS THE RADIAL COMPONENT OF THE WATER VELOCITY AND IS POSITIVE TOWARD THE SHAFT CENTERLINE.
- $V_{tr}$  IS THE TRANSVERSE COMPONENT OF THE WATER VELOCITY AND IS THE VECTOR SUM OF  $V_t$  AND  $V_r$ .

THE VECTOR SHOWN IN THE DIAGRAM IS IN THE DIRECTION OF  $V_{tr}$  WITH A MAGNITUDE EQUAL TO  $V_{tr}/V$ .

THE VELOCITY MEASUREMENTS WERE MADE IN A PLANE WHICH IS PERPENDICULAR TO THE CENTERLINE OF THE PROPELLER SHAFT AND INTERSECTS THE SHAFT CENTERLINE 0.57 FT FWD OF STA 19.

TABLE OF COMPONENT RATIOS

POSITION NUMBER	$V_x/V$	$V_t/V$	$V_r/V$
101	0.986	0.043	-0.074
102	1.015	-0.143	-0.112
103	1.027	-0.145	-0.094
104	1.031	-0.178	0
105	1.044	-0.121	0.089
106	1.037	0	0.133
107	1.041	0.121	0.088
108	1.033	0.169	-0.018
109	1.046	0.187	-0.083
110	1.016	0.098	-0.072
201	0.984	-0.043	-0.100
202	1.013	-0.093	-0.132
203	1.019	-0.134	-0.084
204	1.024	-0.158	-0.068
205	1.023	-0.103	0.103
206	1.024	0	0.145
207	1.023	0.103	0.103
208	1.029	0.160	0
209	1.019	0.164	-0.138
210	0.892	0.072	-0.111
301	0.939	-0.050	-0.154
302	0.984	-0.101	-0.152
303	1.016	-0.130	-0.105
304	1.018	-0.149	0.018
305	1.023	-0.100	0.100
306	1.016	0	0.140
307	1.014	0.098	0.098
308	1.024	0.158	0.009
309	0.898	0.116	-0.127
310	0.771	0.045	-0.111

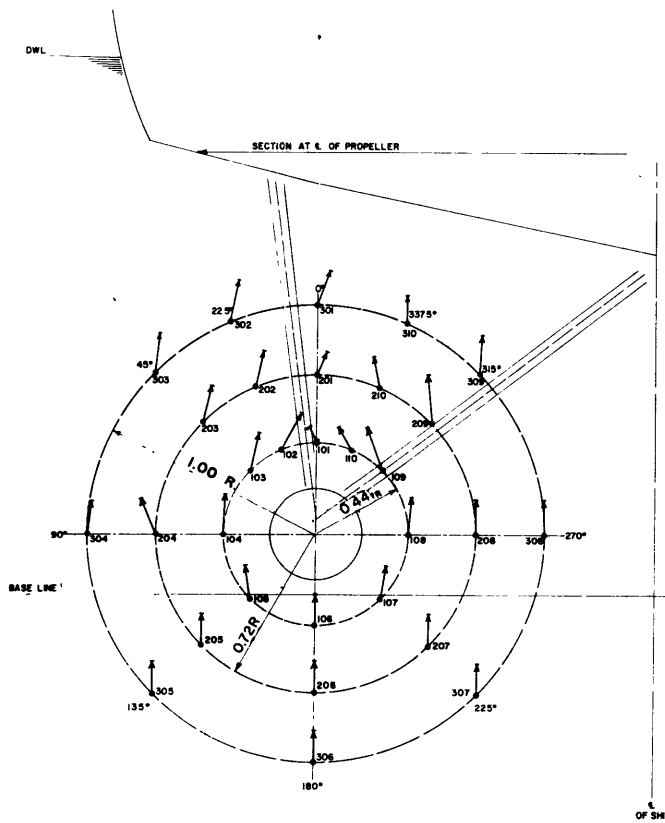


Figure 4 - Wake Velocity Diagram and Test Data, Model 3869

VELOCITY SURVEY IN WAY OF THE PROPELLER	
TWIN-SCREW SHIPS	
MILITARY TYPE	
MODEL 3870-1	
MODEL DIMENSIONS	
LENGTH (LWL)	20.759 FT
BEAM	2.197 FT
DRAFT	.702 FT
DISPLACEMENT	.474 TONS F.W.
PROPELLER DIAMETER	.673 FT
SPEED	7.00 KT
TEST 9	
AUGUST 1944	

- $r/R$  IS THE DISTANCE FROM THE PROPELLER AXIS ( $r$ ) EXPRESSED AS A RATIO OF THE PROPELLER RADIUS ( $R$ ).
- $\theta$  IS THE ANGLE MEASURED FROM THE TOP OF THE PROPELLER DISK IN A COUNTERCLOCKWISE DIRECTION.
- $V$  IS THE SHIP SPEED.
- $V_x$  IS THE LONGITUDINAL (NORMAL TO THE PLANE OF SURVEY) COMPONENT OF THE WATER VELOCITY AND IS POSITIVE IN THE ASTERN DIRECTION.
- $V_t$  IS THE TANGENTIAL COMPONENT OF THE WATER VELOCITY AND IS POSITIVE IN THE COUNTERCLOCKWISE DIRECTION.
- $V_r$  IS THE RADIAL COMPONENT OF THE WATER VELOCITY AND IS POSITIVE TOWARD THE SHAFT CENTERLINE.
- $V_{tr}$  IS THE TRANSVERSE COMPONENT OF THE WATER VELOCITY AND IS THE VECTOR SUM OF  $V_t$  AND  $V_r$ .

THE VECTOR SHOWN IN THE DIAGRAM IS IN THE DIRECTION OF  $V_{tr}$  WITH A MAGNITUDE EQUAL TO  $V_{tr}/V$ .

THE VELOCITY MEASUREMENTS WERE MADE IN A PLANE WHICH IS PERPENDICULAR TO THE CENTERLINE OF THE PROPELLER SHAFT AND INTERSECTS THE SHAFT CENTERLINE 0.57 FT FWD OF STA 19.

TABLE OF COMPONENT RATIOS

POSITION NUMBER	$V_x/V$	$V_t/V$	$V_r/V$
101	1.004	-0.115	-0.112
102	0.998	-0.143	-0.090
103	1.000	-0.182	-0.067
104	1.013	-0.194	0.009
105	1.014	-0.143	0.092
106	1.016	-0.018	0.117
107	1.014	0.092	0.079
108	1.005	0.139	-0.009
109	0.995	0.147	-0.072
110	0.904	-0.184	-0.187
201	0.936	-0.108	-0.137
202	0.997	-0.132	-0.113
203	1.012	-0.150	-0.073
204	1.006	-0.165	0.022
205	1.010	-0.108	0.108
206	1.009	-0.009	0.129
207	1.003	0.085	0.098
208	1.006	0.129	0
209	0.898	0.128	-0.091
210	0.708	0.144	-0.013
301	0.831	-0.052	-0.144
302	0.951	-0.117	-0.120
303	0.981	-0.149	-0.077
304	1.012	-0.147	0.022
305	1.012	-0.098	0.098
306	1.007	-0.009	0.134
307	1.006	0.085	0.098
308	1.003	0.138	0.009
309	0.950	0.116	-0.116
310	0.816	0.131	-0.091

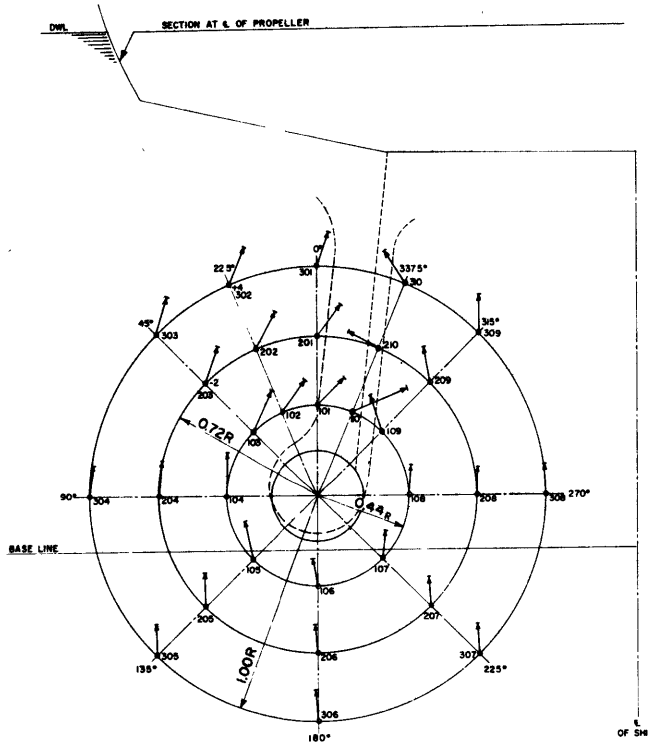


Figure 5 - Wake Velocity Diagram and Test Data, Model 3870-1

VELOCITY SURVEY IN WAY OF THE PROPELLER	
TWIN-CREW SHEPS	
MILITARY TYPE	
MODEL 3878	
MODEL DIMENSIONS	
LENGTH (LWL)	20.789 FT
BEAM	2.318 FT
DRAFT	.708 FT
DISPLACEMENT	.474 TONS F.W.
PROPELLER DIAMETER	.873 FT
SPEED	7.0 KT
TEST 0	
SEPTEMBER 1944	

- $r/R$  IS THE DISTANCE FROM THE PROPELLER AXIS ( $r$ ) EXPRESSED AS A RATIO OF THE PROPELLER RADIUS ( $R$ ).
- $\theta$  IS THE ANGLE MEASURED FROM THE TOP OF THE PROPELLER DISK IN A COUNTERCLOCKWISE DIRECTION.
- $V$  IS THE SHIP SPEED.
- $V_x$  IS THE LONGITUDINAL (NORMAL TO THE PLANE OF SURVEY) COMPONENT OF THE WATER VELOCITY AND IS POSITIVE IN THE AFTERN DIRECTION.
- $V_t$  IS THE TANGENTIAL COMPONENT OF THE WATER VELOCITY AND IS POSITIVE IN THE COUNTERCLOCKWISE DIRECTION.
- $V_r$  IS THE RADIAL COMPONENT OF THE WATER VELOCITY AND IS POSITIVE TOWARD THE SHAFT CENTERLINE.
- $V_{tr}$  IS THE TRANSVERSE COMPONENT OF THE WATER VELOCITY AND IS THE VECTOR SUM OF  $V_t$  AND  $V_r$ .

THE VECTOR SHOWN IN THE DIAGRAM IS IN THE DIRECTION OF  $V_{tr}$  WITH A MAGNITUDE EQUAL TO  $V_{tr}/V$ .

THE VELOCITY MEASUREMENTS WERE MADE IN A PLANE WHICH IS PERPENDICULAR TO THE CENTERLINE OF THE PROPELLER SHAFT AND INTERSECTS THE SHAFT CENTERLINE .57 FT FWD OF STA 19.

TABLE OF COMPONENT RATIOS

POSITION NUMBER	$V_x/V$	$V_t/V$	$V_r/V$
101	1.052	-0.046	-0.033
102	1.026	-0.151	-0.110
103	1.012	-0.149	-0.086
104	1.020	-0.185	0.009
105	1.028	-0.125	0.087
106	1.027	0	0.123
107	1.030	0.118	0.090
108	1.021	0.158	-0.018
109	0.999	0.137	-0.095
110	0.827	0.111	-0.096
201	1.008	-0.053	-0.125
202	1.023	-0.163	-0.133
203	1.011	-0.142	-0.079
204	1.016	-0.158	0.022
205	1.017	-0.105	0.105
206	1.016	0	0.144
207	1.018	0.108	0.095
208	1.017	0.153	-0.009
209	0.985	0.123	-0.119
210	0.861	0.087	-0.079
301	0.953	-0.071	-0.139
302	0.972	-0.167	-0.142
303	1.013	-0.136	-0.086
304	1.014	-0.153	0.022
305	1.017	-0.105	0.105
306	1.010	0	0.143
307	1.017	0.102	0.102
308	1.010	0.147	0
309	0.811	0.113	-0.118
310	0.730	0.070	-0.107

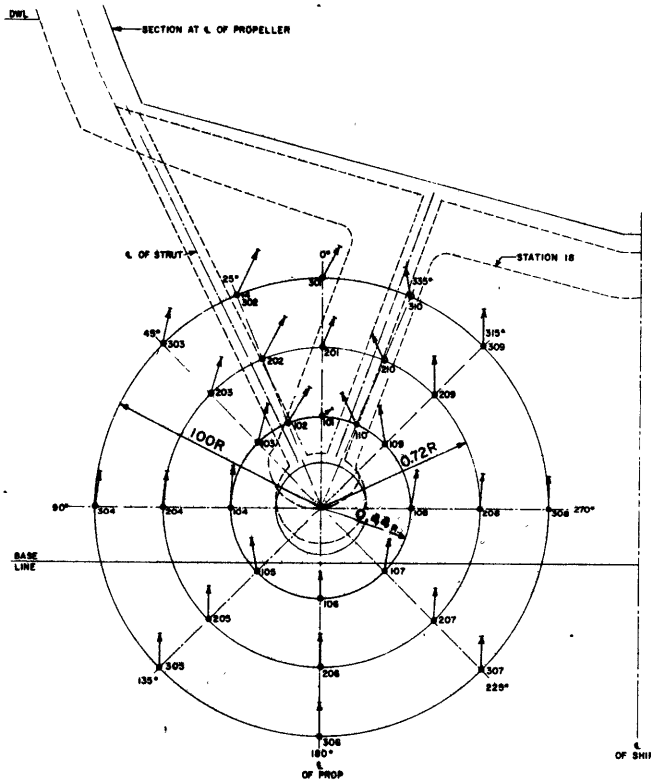


Figure 6 - Wake Velocity Diagram and Test Data, Model 3878

VELOCITY SURVEY IN WAY OF THE PROPELLER	
TWIN SCREW SHIPS	
MILITARY TYPE	
MODEL 3884	
MODEL DIMENSIONS	
LENGTH (LWL)	20.00 FT
BEAM	2.197 FT
DRAFT	.711 FT
DISPLACEMENT	.448 TONS F.W.
PROPELLER DIAMETER	.665 FT
SPEED	7.00 KT
TEST 0	
OCTOBER 1944	

- $r/R$  IS THE DISTANCE FROM THE PROPELLER AXIS ( $r$ ) EXPRESSED AS A RATIO OF THE PROPELLER RADIUS ( $R$ ).
- $\theta$  IS THE ANGLE MEASURED FROM THE TOP OF THE PROPELLER DISK IN A COUNTERCLOCKWISE DIRECTION.
- $V$  IS THE SHIP SPEED.
- $V_x$  IS THE LONGITUDINAL (NORMAL TO THE PLANE OF SURVEY) COMPONENT OF THE WATER VELOCITY AND IS POSITIVE IN THE ASTERN DIRECTION.
- $V_t$  IS THE TANGENTIAL COMPONENT OF THE WATER VELOCITY AND IS POSITIVE IN THE COUNTERCLOCKWISE DIRECTION.
- $V_r$  IS THE RADIAL COMPONENT OF THE WATER VELOCITY AND IS POSITIVE TOWARD THE SHAFT CENTERLINE.
- $V_{tr}$  IS THE TRANSVERSE COMPONENT OF THE WATER VELOCITY AND IS THE VECTOR SUM OF  $V_t$  AND  $V_r$ .

THE VECTOR SHOWN IN THE DIAGRAM IS IN THE DIRECTION OF  $V_{tr}$  WITH A MAGNITUDE EQUAL TO  $V_{tr}/V$ .

THE VELOCITY MEASUREMENTS WERE MADE IN A PLANE WHICH IS PERPENDICULAR TO THE CENTERLINE OF THE PROPELLER SHAFT AND INTERSECTS THE SHAFT CENTERLINE 0.57 FT FWD OF STA 19.

TABLE OF COMPONENT RATIOS

POSITION NUMBER	$V_x/V$	$V_t/V$	$V_r/V$
101	0.962	0	-0.017
102	1.041	-0.125	-0.097
103	1.038	-0.153	-0.102
104	1.046	-0.169	-0.099
105	1.038	-0.113	0.074
106	1.040	0.009	0.105
107	1.042	0.124	0.072
108	1.030	0.160	-0.027
109	1.039	0.139	-0.124
110	1.024	0.099	-0.072
201	0.931	-0.016	-0.094
202	1.020	-0.103	-0.129
203	1.027	-0.132	-0.081
204	1.027	-0.146	0.009
205	1.024	-0.100	0.100
206	1.020	0	0.131
207	1.024	0.109	0.097
208	1.022	0.158	-0.009
209	0.926	0.114	-0.102
210	0.978	0.074	-0.133
301	0.899	-0.040	-0.131
302	1.001	-0.105	-0.139
303	1.022	-0.132	-0.093
304	1.021	-0.149	0.014
305	1.014	-0.086	0.098
306	1.015	0	0.131
307	1.017	0.105	0.092
308	1.021	0.158	0
309	0.964	0.075	-0.142
310	0.859	0.035	-0.141

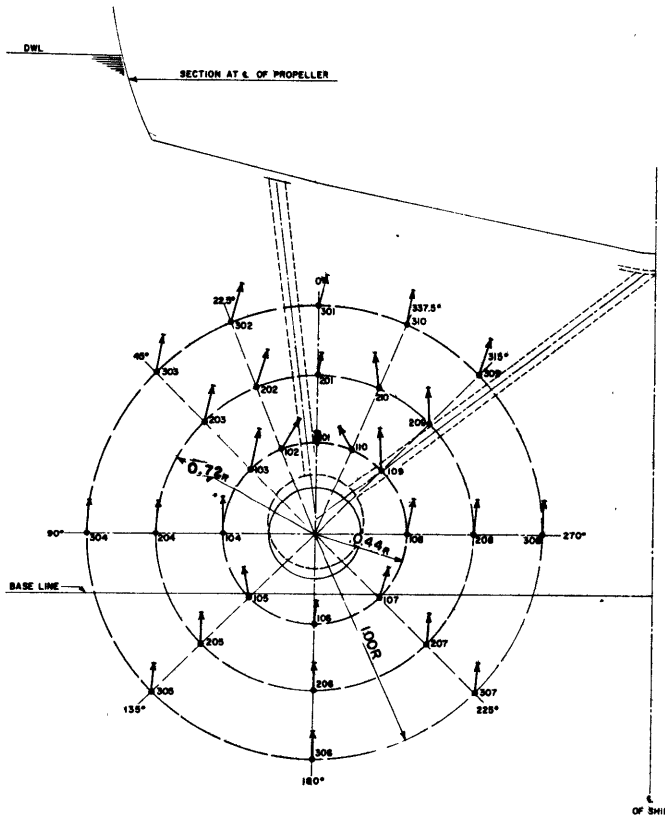


Figure 7 - Wake Velocity Diagram and Test Data, Model 3884

VELOCITY SURVEY IN WAY OF THE PROPELLER TWIN SCREW SHIPS MILITARY TYPE MODEL 4048	
MODEL DIMENSIONS	
LENGTH (LWL)	20.60 FT
BEAM	2.070 FT
DRAFT	.690 FT
DISPLACEMENT	.368 TONS F. W.
PROPELLER DIAMETER	.588 FT
SPEED	6.47 KT
TEST 18 JUNE 1955	

- $r/R$  IS THE DISTANCE FROM THE PROPELLER AXIS ( $r$ ) EXPRESSED AS A RATIO OF THE PROPELLER RADIUS ( $R$ ).
- $\theta$  IS THE ANGLE MEASURED FROM THE TOP OF THE PROPELLER DISK IN A COUNTERCLOCKWISE DIRECTION.
- $V$  IS THE SHIP SPEED.
- $V_x$  IS THE LONGITUDINAL (NORMAL TO THE PLANE OF SURVEY) COMPONENT OF THE WATER VELOCITY AND IS POSITIVE IN THE ASTERN DIRECTION.
- $V_t$  IS THE TANGENTIAL COMPONENT OF THE WATER VELOCITY AND IS POSITIVE IN THE COUNTERCLOCKWISE DIRECTION.
- $V_r$  IS THE RADIAL COMPONENT OF THE WATER VELOCITY AND IS POSITIVE TOWARD THE SHAFT CENTERLINE.
- $V_{tr}$  IS THE TRANSVERSE COMPONENT OF THE WATER VELOCITY AND IS THE VECTOR SUM OF  $V_t$  AND  $V_r$ .

THE VECTOR SHOWN IN THE DIAGRAM IS IN THE DIRECTION OF  $V_{tr}$  WITH A MAGNITUDE EQUAL TO  $V_{tr}/V$ .

THE VELOCITY MEASUREMENTS WERE MADE IN A PLANE WHICH IS PERPENDICULAR TO THE CENTERLINE OF THE PROPELLER SHAFT AND INTERSECTS THE SHAFT CENTERLINE AT STA 19.

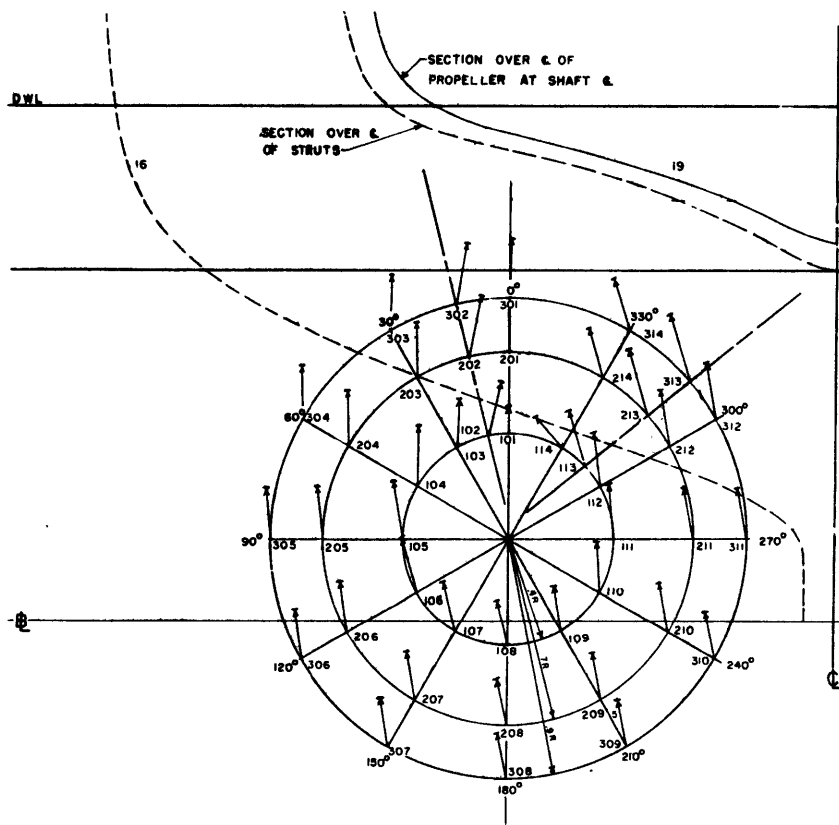


TABLE OF COMPONENT RATIOS

POSITION NUMBER	$V_x/V$	$V_t/V$
101	0.942	0.001
102	1.048	-0.073
103	1.041	-0.092
104	1.051	-0.167
105	1.050	-0.187
106	1.051	-0.172
107	1.052	-0.117
108	1.048	-0.033
109	1.046	0.053
110	1.048	0.134
111	1.041	0.173
112	1.036	0.156
113	0.994	0.162
114	1.041	0.119
201	1.015	0.002
202	1.036	-0.078
203	1.030	-0.084
204	1.032	-0.147
205	1.035	-0.168
206	1.038	-0.155
207	1.038	-0.104
208	1.032	-0.034
209	1.030	0.049
210	1.025	0.118
211	1.017	0.164
212	1.004	0.169
213	0.984	0.199
214	0.983	0.118
301	0.941	-0.004
302	1.030	-0.079
303	1.030	-0.091
304	1.029	-0.146
305	1.030	-0.166
306	1.031	-0.148
307	1.034	-0.103
308	1.031	-0.031
309	1.024	0.048
310	1.021	0.116
311	1.007	0.160
312	0.988	0.172
313	0.975	0.204
314	0.926	0.129

Figure 8 - Wake Velocity Diagram and Test Data, Model 4048

VELOCITY SURVEY IN WAY OF THE PROPELLER TWIN SCREW SHIPS MILITARY TYPE MODEL 4051	
<b>MODEL DIMENSIONS</b>	
LENGTH (LWL)	20.00 FT
BEAM	2.01 FT
DRAFT	.588 FT
DISPLACEMENT	.323 TONS F. W.
PROPELLER DIAMETER	.585 FT
SPEED	7.48 KT
TEST 0 JUNE 1955	

- $r/R$  IS THE DISTANCE FROM THE PROPELLER AXIS ( $r$ ) EXPRESSED AS A RATIO OF THE PROPELLER RADIUS ( $R$ ).
- $\theta$  IS THE ANGLE MEASURED FROM THE TOP OF THE PROPELLER DISK IN A COUNTERCLOCKWISE DIRECTION.
- $V$  IS THE SHIP SPEED.
- $V_x$  IS THE LONGITUDINAL (NORMAL TO THE PLANE OF SURVEY) COMPONENT OF THE WATER VELOCITY AND IS POSITIVE IN THE ASTERN DIRECTION.
- $V_t$  IS THE TANGENTIAL COMPONENT OF THE WATER VELOCITY AND IS POSITIVE IN THE COUNTERCLOCKWISE DIRECTION.
- $V_r$  IS THE RADIAL COMPONENT OF THE WATER VELOCITY AND IS POSITIVE TOWARD THE SHAFT CENTERLINE.
- $V_{tr}$  IS THE TRANSVERSE COMPONENT OF THE WATER VELOCITY AND IS THE VECTOR SUM OF  $V_t$  AND  $V_r$ .

THE VECTOR SHOWN IN THE DIAGRAM IS IN THE DIRECTION OF  $V_{tr}$  WITH A MAGNITUDE EQUAL TO  $V_{tr}/V$ .

THE VELOCITY MEASUREMENTS WERE MADE IN A PLANE WHICH IS PERPENDICULAR TO THE CENTERLINE OF THE PROPELLER SHAFT AND INTERSECTS THE SHAFT CENTERLINE 24 FT FWD OF AP.

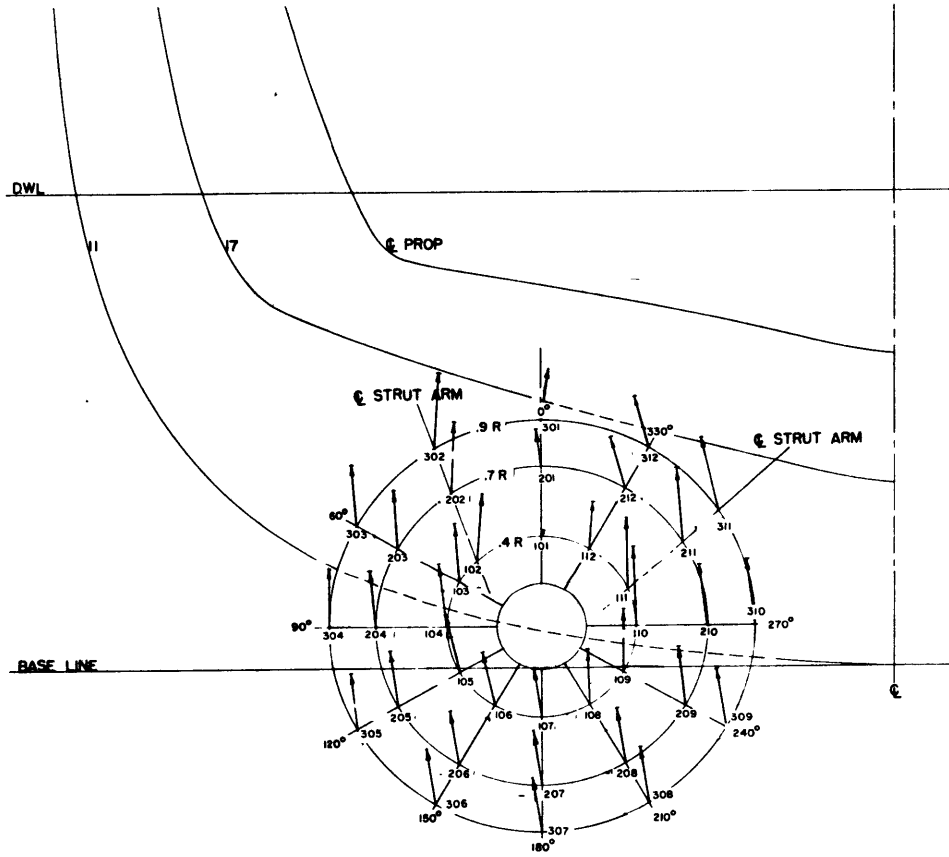


TABLE OF COMPONENT RATIOS

POSITION NUMBER	$V_x/V$	$V_t/V$
101	0.998	-0.012
102	1.054	-0.158
103	1.043	-0.152
104	1.057	-0.193
105	1.061	-0.177
106	1.062	-0.111
107	1.066	-0.022
108	1.060	0.085
109	1.021	0.168
110	1.040	0.205
111	1.053	0.218
112	1.041	0.068
201	0.949	0.014
202	1.035	-0.115
203	1.038	-0.148
204	1.045	-0.178
205	1.044	-0.160
206	1.046	-0.110
207	1.044	0.029
208	1.047	0.067
209	1.046	0.152
210	1.044	0.193
211	1.008	0.216
212	0.986	0.119
301	0.969	-0.014
302	1.029	-0.129
303	1.043	-0.145
304	1.045	-0.175
305	1.045	-0.153
306	1.045	-0.108
307	1.042	-0.026
308	1.042	0.061
309	1.044	0.141
310	1.055	0.212
311	0.979	0.214
312	0.917	0.119

Figure 9 - Wake Velocity Diagram and Test Data, Model 4051

VELOCITY SURVEY IN WAY OF THE PROPELLER TWIN SCREW SHIPS MILITARY TYPE MODEL 4569-1	
<b>MODEL DIMENSIONS</b>	
LENGTH (LWL)	20.47 FT
BEAM	2.09 FT
DRAFT	.658 FT
DISPLACEMENT	.340 TONS F.W.
PROPELLER DIAMETER	.585 FT
SPEED	7.15 KT
TEST 15 MARCH 1956	

$r/R$  IS THE DISTANCE FROM THE PROPELLER AXIS ( $r$ ) EXPRESSED AS A RATIO OF THE PROPELLER RADIUS ( $R$ ).

$\theta$  IS THE ANGLE MEASURED FROM THE TOP OF THE PROPELLER DISK IN A COUNTERCLOCKWISE DIRECTION.

$V$  IS THE SHIP SPEED.

$V_x$  IS THE LONGITUDINAL (NORMAL TO THE PLANE OF SURVEY) COMPONENT OF THE WATER VELOCITY AND IS POSITIVE IN THE ASTERN DIRECTION.

$V_t$  IS THE TANGENTIAL COMPONENT OF THE WATER VELOCITY AND IS POSITIVE IN THE COUNTERCLOCKWISE DIRECTION.

$V_r$  IS THE RADIAL COMPONENT OF THE WATER VELOCITY AND IS POSITIVE TOWARD THE SHAFT CENTERLINE.

$V_{tr}$  IS THE TRANSVERSE COMPONENT OF THE WATER VELOCITY AND IS THE VECTOR SUM OF  $V_t$  AND  $V_r$ .

THE VECTOR SHOWN IN THE DIAGRAM IS IN THE DIRECTION OF  $V_{tr}$  WITH A MAGNITUDE EQUAL TO  $V_{tr}/V$ .

THE VELOCITY MEASUREMENTS WERE MADE IN A PLANE WHICH IS PERPENDICULAR TO THE CENTERLINE OF THE PROPELLER SHAFT AND INTERSECTS THE SHAFT CENTERLINE AT STA 19.

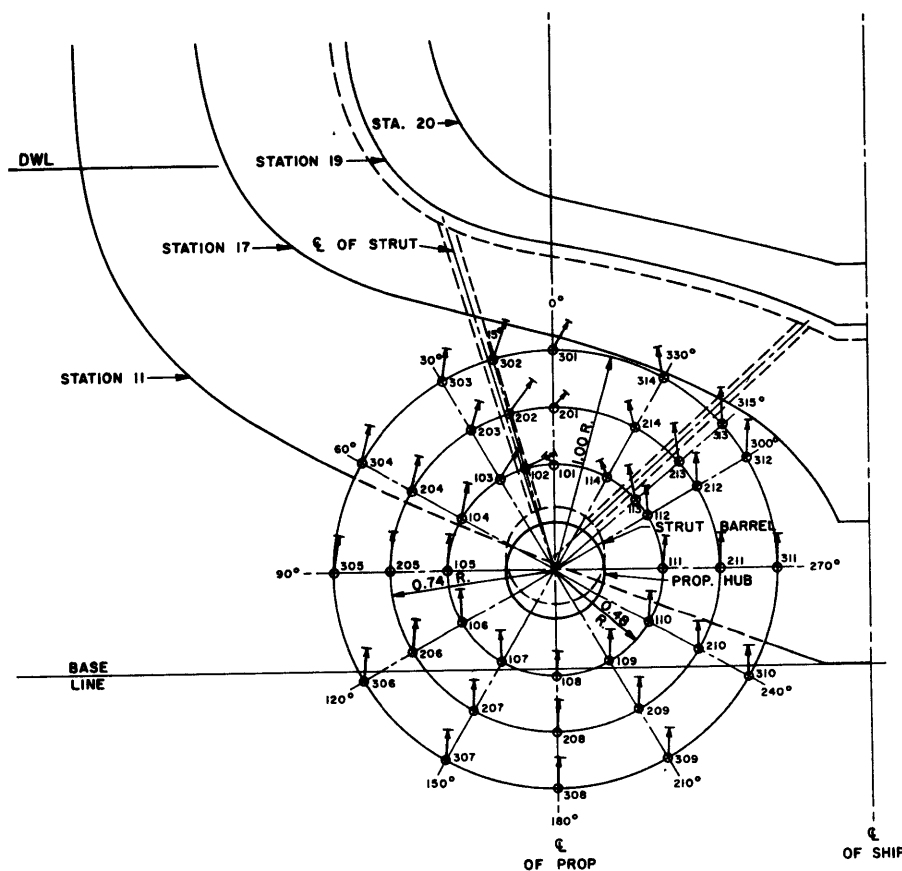


TABLE OF COMPONENT RATIOS

POSITION NUMBER	$V_x/V$	$V_t/V$	$V_r/V$
101	0.930	0.030	-0.040
102	0.940	-0.160	-0.030
103	1.040	-0.140	-0.070
104	1.030	-0.160	-0.040
105	1.040	-0.180	0.020
106	1.050	-0.140	0.080
107	1.050	-0.080	0.120
108	1.050	0.010	0.140
109	1.050	0.080	0.120
110	1.050	0.140	0.070
111	1.040	0.160	0
112	1.040	0.130	-0.060
113	1.040	0.150	-0.080
114	1.050	0.070	-0.060
201	0.990	-0.060	-0.080
202	0.960	-0.130	-0.120
203	1.030	-0.100	-0.090
204	1.030	-0.150	-0.040
205	1.040	-0.160	0.030
206	1.050	-0.130	0.090
207	1.050	-0.070	0.130
208	1.050	0.010	0.140
209	1.040	0.080	0.120
210	1.040	0.130	0.070
211	1.030	0.160	-0.010
212	1.020	0.140	-0.080
213	1.040	0.160	-0.100
214	0.970	0.100	-0.110
301	0.930	-0.080	-0.140
302	0.890	-0.090	-0.140
303	1.020	-0.060	-0.120
304	1.030	-0.160	-0.050
305	1.040	-0.150	0.020
306	1.040	-0.120	0.090
307	1.040	-0.070	0.130
308	1.040	0	0.140
309	1.040	0.080	0.120
310	1.040	0.130	0.070
311	1.050	0.160	0
312	1.010	0.140	-0.100
313	1.000	0.140	-0.110
314	0.920	0.100	-0.130

Figure 10 - Wake Velocity Diagram and Test Data, Model 4569-1



VELOCITY SURVEY IN WAY OF THE PROPELLER TWIN SCREW SHIPS MILITARY TYPE MODEL 4659	
MODEL DIMENSIONS	
LENGTH (LWL)	26.47 FT
BEAM	2.72 FT
DRAFT	.823 FT
DISPLACEMENT	.767 TONS F.W.
PROPELLER DIAMETER	.650 FT
SPEED	5.87 KT
TEST 15 FEBRUARY 1958	

- $r/R$  IS THE DISTANCE FROM THE PROPELLER AXIS ( $r$ ) EXPRESSED AS A RATIO OF THE PROPELLER RADIUS ( $R$ ).
- $\theta$  IS THE ANGLE MEASURED FROM THE TOP OF THE PROPELLER DISK IN A COUNTERCLOCKWISE DIRECTION.
- $V$  IS THE SHIP SPEED.
- $V_x$  IS THE LONGITUDINAL (NORMAL TO THE PLANE OF SURVEY) COMPONENT OF THE WATER VELOCITY AND IS POSITIVE IN THE ASTERN DIRECTION.
- $V_t$  IS THE TANGENTIAL COMPONENT OF THE WATER VELOCITY AND IS POSITIVE IN THE COUNTERCLOCKWISE DIRECTION.
- $V_r$  IS THE RADIAL COMPONENT OF THE WATER VELOCITY AND IS POSITIVE TOWARD THE SHAFT CENTERLINE.
- $V_{tr}$  IS THE TRANSVERSE COMPONENT OF THE WATER VELOCITY AND IS THE VECTOR SUM OF  $V_t$  AND  $V_r$ .

THE VECTOR SHOWN IN THE DIAGRAM IS IN THE DIRECTION OF  $V_{tr}$  WITH A MAGNITUDE EQUAL TO  $V_{tr}/V$ .

THE VELOCITY MEASUREMENTS WERE MADE IN A PLANE WHICH IS PERPENDICULAR TO THE CENTERLINE OF THE PROPELLER SHAFT AND INTERSECTS THE SHAFT CENTERLINE 4.5 FT FWD OF STA 19.

TABLE OF COMPONENT RATIOS

POSITION NUMBER	$V_x/V$	$V_t/V$	$V_r/V$
101	0.785	-0.023	-0.021
102	0.859	-0.082	-0.048
103	0.965	-0.091	-0.099
104	0.992	-0.101	-0.089
105	1.025	-0.088	-0.046
106	1.022	-0.057	0.011
107	1.019	-0.008	0.042
108	1.019	0.047	0.075
109	1.019	0.100	0.088
110	0.988	0.127	0.081
111	0.974	0.124	0.045
112	0.962	0.095	0.002
113	0.903	0.101	-0.011
114	0.816	0.043	0.004
201	0.826	-0.034	-0.073
202	0.812	-0.067	-0.076
203	0.918	-0.081	-0.107
204	0.976	-0.101	-0.088
205	1.020	-0.079	-0.040
206	1.018	-0.054	0.010
207	1.015	-0.002	0.061
208	1.011	0.051	0.089
209	1.009	0.093	0.095
210	0.993	0.124	0.081
211	0.973	0.119	0.043
212	0.916	0.074	-0.001
213	0.813	0.100	-0.047
214	0.814	0.031	-0.057
301	0.795	-0.041	-0.079
302	0.773	-0.061	-0.101
303	0.861	-0.070	-0.104
304	0.973	-0.100	-0.084
305	1.030	-0.071	-0.036
306	1.007	-0.052	0.017
307	1.002	-0.003	0.063
308	1.007	0.046	0.091
309	1.010	0.090	0.098
310	1.001	0.118	0.078
311	0.975	0.121	0.040
312	0.931	0.087	-0.001
313	0.819	0.099	-0.041
314	0.722	0.046	-0.054

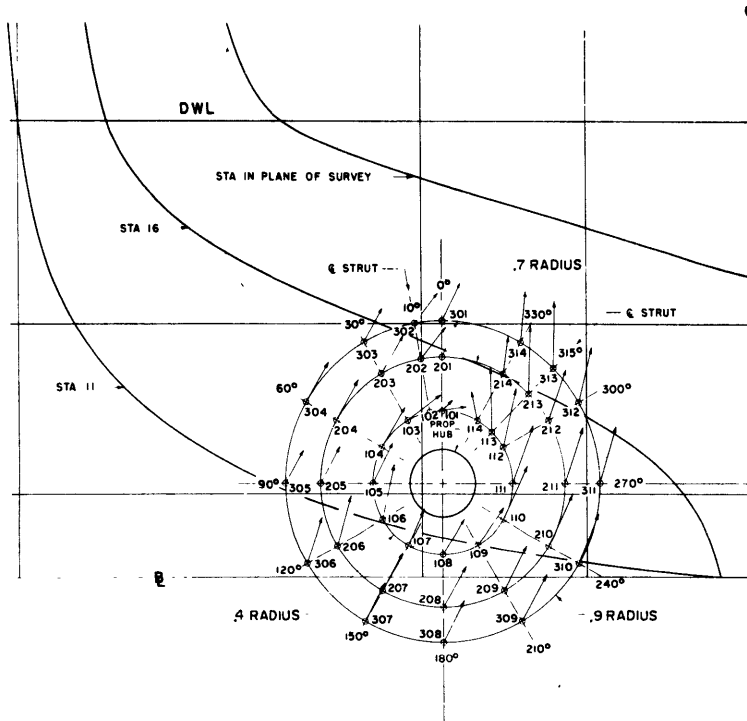


Figure 11 - Wake Velocity Diagram and Test Data, Model 4659

VELOCITY SURVEY IN WAY OF THE PROPELLER TWIN SCREW SHIPS MILITARY TYPE MODEL 4711	
<b>MODEL DIMENSIONS</b>	
LENGTH (LWL)	22.440 FT
BEAM	2.363 FT
DRAFT	.769 FT
DISPLACEMENT	.586 TONS F. W.
PROPELLER DIAMETER	.623 FT
SPEED	6.21 KT
TEST 22 DECEMBER 1961	

- $r/R$  IS THE DISTANCE FROM THE PROPELLER AXIS ( $r$ ) EXPRESSED AS A RATIO OF THE PROPELLER RADIUS ( $R$ )
- $\theta$  IS THE ANGLE MEASURED FROM THE TOP OF THE PROPELLER DISK IN A COUNTERCLOCKWISE DIRECTION.
- $V$  IS THE SHIP SPEED.
- $V_x$  IS THE LONGITUDINAL (NORMAL TO THE PLANE OF SURVEY) COMPONENT OF THE WATER VELOCITY AND IS POSITIVE IN THE ASTERN DIRECTION.
- $V_t$  IS THE TANGENTIAL COMPONENT OF THE WATER VELOCITY AND IS POSITIVE IN THE COUNTERCLOCKWISE DIRECTION.
- $V_r$  IS THE RADIAL COMPONENT OF THE WATER VELOCITY AND IS POSITIVE TOWARD THE SHAFT CENTERLINE.
- $V_{tr}$  IS THE TRANSVERSE COMPONENT OF THE WATER VELOCITY AND IS THE VECTOR SUM OF  $V_t$  AND  $V_r$ .

THE VECTOR SHOWN IN THE DIAGRAM IS IN THE DIRECTION OF  $V_{tr}$  WITH A MAGNITUDE EQUAL TO  $V_{tr}/V$ .

THE VELOCITY MEASUREMENTS WERE MADE IN A PLANE WHICH IS PERPENDICULAR TO THE CENTERLINE OF THE PROPELLER SHAFT AND INTERSECTS THE SHAFT CENTERLINE 22.2 FT FWD OF A. P.

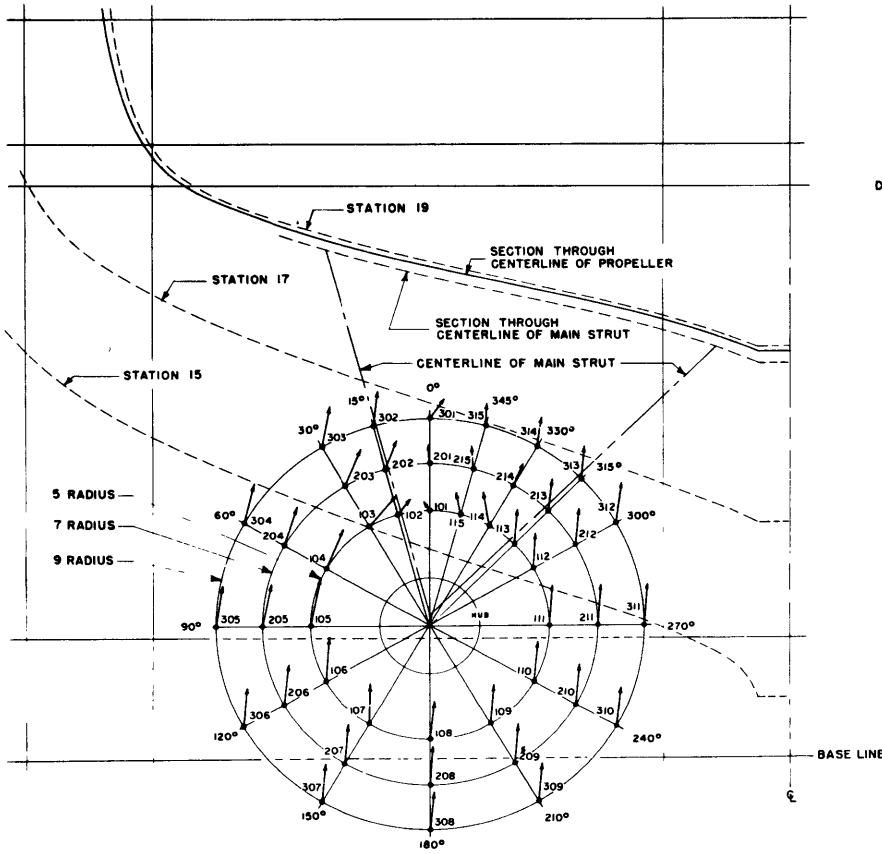


**TABLE OF COMPONENT RATIOS**

POSITION NUMBER	$V_x/V$	$V_t/V$	$V_r/V$
101	0.880	0.020	-0.030
102	0.830	-0.050	-0.040
103	0.970	-0.120	-0.040
104	1.000	-0.140	-0.020
105	1.010	-0.150	0.030
106	1.020	-0.120	0.080
D. W. L. 107	1.010	-0.060	0.110
108	1.010	0.010	0.120
109	1.010	0.070	0.100
110	0.990	0.120	0.050
111	0.980	0.130	-0.010
112	0.960	0.100	-0.060
113	0.940	0.070	-0.080
114	0.880	0.070	-0.080
115	0.920	0.030	-0.060
201	0.820	0	-0.060
202	0.830	-0.060	-0.080
203	0.960	-0.100	-0.080
204	1.000	-0.130	-0.030
205	1.000	-0.140	0.030
206	1.000	-0.110	0.080
207	1.000	-0.060	0.110
208	1.000	0.010	0.120
209	1.000	0.070	0.100
210	0.990	0.120	0.050
211	0.980	0.130	-0.010
212	0.940	0.100	-0.070
213	0.910	0.060	-0.080
214	0.890	0.010	-0.070
215	0.850	0.030	-0.070
301	0.850	-0.040	-0.070
302	0.860	-0.040	-0.100
303	0.960	-0.090	-0.100
304	0.990	-0.130	-0.040
305	0.990	-0.130	0.020
306	1.000	-0.100	0.080
307	0.990	-0.050	0.110
308	0.990	0.010	0.120
309	0.990	0.070	0.100
310	0.980	0.120	0.050
311	0.980	0.140	-0.010
312	0.940	0.100	-0.080
313	0.900	0.070	-0.080
314	0.880	0.030	-0.090
315	0.770	0.010	-0.070

Figure 12 - Wake Velocity Diagram and Test Data, Model 4711-1

VELOCITY SURVEY IN WAY OF THE PROPELLER TWIN SCREW SHIPS MILITARY TYPE MODEL 4921	
MODEL DIMENSIONS	
LENGTH (LWL)	22.51 FT
BEAM	2.369 FT
DRAFT	.844 FT
DISPLACEMENT	.635 TONS F.W.
PROPELLER DIAMETER	.520 FT
SPEED	5.91 KT
TEST 9 JULY 1962	

- $r/R$  IS THE DISTANCE FROM THE PROPELLER AXIS ( $r$ ) EXPRESSED AS A RATIO OF THE PROPELLER RADIUS ( $R$ ).
- $\theta$  IS THE ANGLE MEASURED FROM THE TOP OF THE PROPELLER DISK IN A COUNTERCLOCKWISE DIRECTION.
- $V$  IS THE SHIP SPEED.
- $V_x$  IS THE LONGITUDINAL (NORMAL TO THE PLANE OF SURVEY) COMPONENT OF THE WATER VELOCITY AND IS POSITIVE IN THE ASTERN DIRECTION.
- $V_t$  IS THE TANGENTIAL COMPONENT OF THE WATER VELOCITY AND IS POSITIVE IN THE COUNTERCLOCKWISE DIRECTION.
- $V_r$  IS THE RADIAL COMPONENT OF THE WATER VELOCITY AND IS POSITIVE TOWARD THE SHAFT CENTERLINE.
- $V_{tr}$  IS THE TRANSVERSE COMPONENT OF THE WATER VELOCITY AND IS THE VECTOR SUM OF  $V_t$  AND  $V_r$ .

THE VECTOR SHOWN IN THE DIAGRAM IS IN THE DIRECTION OF  $V_{tr}$  WITH A MAGNITUDE EQUAL TO  $V_{tr}/V$ .

THE VELOCITY MEASUREMENTS WERE MADE IN A PLANE WHICH IS PERPENDICULAR TO THE CENTERLINE OF THE PROPELLER SHAFT AND INTERSECTS THE SHAFT CENTERLINE 1.67 FT AFT OF STA 19.

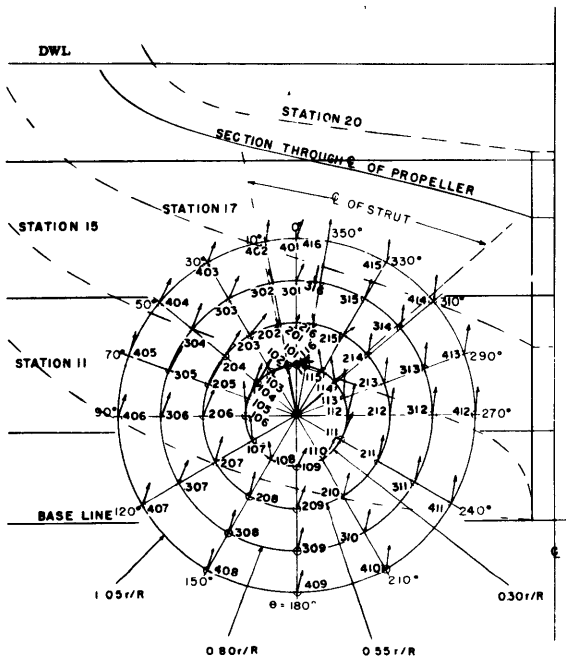


TABLE OF COMPONENT RATIOS

POSITION NUMBER	$V_x/V$	$V_t/V$	$V_r/V$	POSITION NUMBER	$V_x/V$	$V_t/V$	$V_r/V$
101	0.741	-0.026	0.050	301	0.806	-0.035	-0.070
102	0.614	-0.129	0	302	0.822	0.002	-0.060
103	0.996	-0.168	0.030	303	0.879	-0.092	-0.070
104	1.000	-0.174	-0.020	304	0.953	-0.114	-0.030
105	1.000	-0.164	0.020	305	0.977	-0.118	0.020
106	0.999	-0.154	0	306	0.989	-0.103	0.040
107	1.020	-0.103	0.050	307	0.988	-0.072	0.080
108	1.010	-0.038	0.060	308	0.987	-0.026	0.100
109	1.010	0.041	0.080	309	0.975	0.025	0.100
110	1.020	0.101	0.050	310	1.010	0.076	0.080
111	1.010	0.138	0.010	311	0.991	0.111	0.040
112	1.010	0.143	-0.040	312	0.987	0.123	-0.020
113	0.985	0.128	-0.050	313	0.968	0.109	-0.060
114	0.994	0.100	-0.060	314	0.940	0.075	-0.080
115	0.875	0.063	-0.070	315	0.905	0.018	-0.090
116	0.806	0.024	-0.010	316	0.845	0.005	-0.080
201	0.843	-0.011	-0.030	401	0.734	-0.035	-0.080
202	0.830	0.021	-0.020	402	0.736	-0.033	-0.080
203	0.895	-0.108	-0.040	403	0.795	-0.079	-0.060
204	0.966	-0.122	-0.020	404	0.923	-0.110	-0.030
205	0.989	-0.123	0.020	405	0.973	-0.111	0
206	0.995	-0.114	0.040	406	0.980	-0.099	0.040
207	1.000	-0.081	0.080	407	0.979	-0.068	0.080
208	0.998	-0.032	0.100	408	0.981	-0.028	0.100
209	0.993	0.031	0.100	409	0.989	0.026	0.100
210	0.997	0.079	0.080	410	0.989	0.069	0.080
211	0.999	0.116	0.030	411	1.000	0.111	0.050
212	0.991	0.124	-0.020	412	0.980	0.124	-0.020
213	0.972	0.106	-0.060	413	0.979	0.115	-0.060
214	0.943	0.072	-0.070	414	0.949	0.079	-0.090
215	0.928	-0.029	-0.060	415	0.910	0.034	-0.100
216	0.879	0.012	-0.050	416	0.747	0.010	-0.100

Figure 13 - Wake Velocity Diagram and Test Data, Model 4921

VELOCITY SURVEY IN WAY OF THE PROPELLER TWIN SCREW SHIPS MILITARY TYPE MODEL 4892	
<b>MODEL DIMENSIONS</b>	
LENGTH (LWL)	22.57 FT
BEAM	2.856 FT
DRAFT	.799 FT
DISPLACEMENT	.636 TONS F.W.
PROPELLER DIAMETER	.520 FT
SPEED	5.89 KT
TEST 8 SEPTEMBER 1961	

$r/R$  IS THE DISTANCE FROM THE PROPELLER AXIS ( $r$ ) EXPRESSED AS A RATIO OF THE PROPELLER RADIUS ( $R$ ).

$\theta$  IS THE ANGLE MEASURED FROM THE TOP OF THE PROPELLER DISK IN A COUNTERCLOCKWISE DIRECTION.

$V$  IS THE SHIP SPEED.

$V_x$  IS THE LONGITUDINAL (NORMAL TO THE PLANE OF SURVEY) COMPONENT OF THE WATER VELOCITY AND IS POSITIVE IN THE ASTERN DIRECTION.

$V_t$  IS THE TANGENTIAL COMPONENT OF THE WATER VELOCITY AND IS POSITIVE IN THE COUNTERCLOCKWISE DIRECTION.

$V_r$  IS THE RADIAL COMPONENT OF THE WATER VELOCITY AND IS POSITIVE TOWARD THE SHAFT CENTERLINE.

$V_{tr}$  IS THE TRANSVERSE COMPONENT OF THE WATER VELOCITY AND IS THE VECTOR SUM OF  $V_t$  AND  $V_r$ .

THE VECTOR SHOWN IN THE DIAGRAM IS IN THE DIRECTION OF  $V_{tr}$  WITH A MAGNITUDE EQUAL TO  $V_{tr}/V$ .

THE VELOCITY MEASUREMENTS WERE MADE IN A PLANE WHICH IS PERPENDICULAR TO THE CENTERLINE OF THE PROPELLER SHAFT AND INTERSECTS THE SHAFT CENTERLINE 14 FT FWD OF AP.

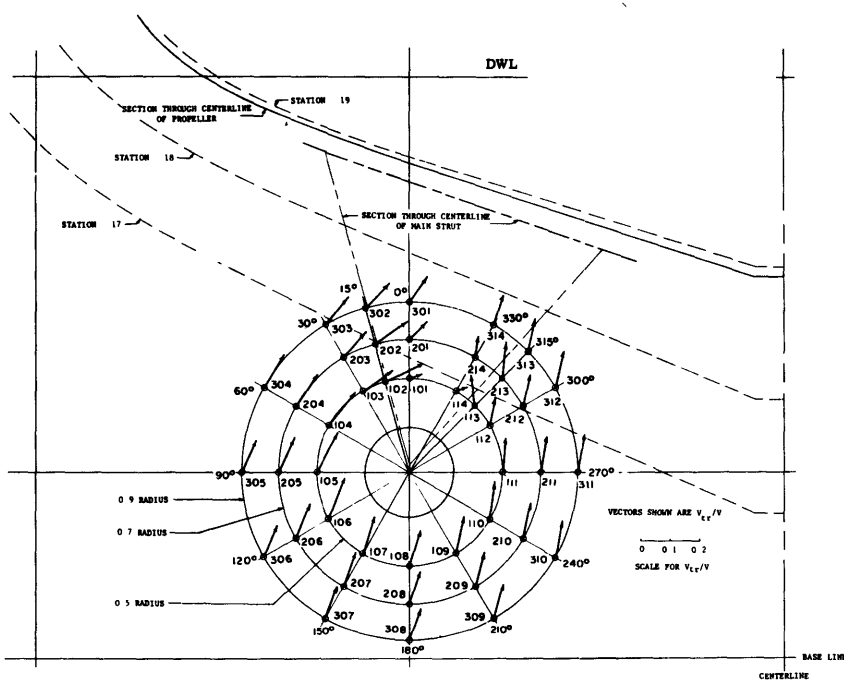


TABLE OF COMPONENT RATIOS

POSITION NUMBER	$V_x/V$	$V_t/V$	$V_r/V$
101	0.842	-0.038	-0.010
102	0.885	-0.144	-0.020
103	0.906	-0.119	-0.010
104	0.951	-0.135	0.030
105	0.984	-0.127	0.070
106	1.002	-0.088	0.110
107	1.012	-0.028	0.130
108	0.988	0.035	0.120
109	0.985	0.088	0.090
110	0.957	0.116	0.040
111	0.929	0.111	-0.010
112	0.899	0.072	0.060
113	0.875	0.081	0.060
114	0.818	-0.024	-0.030
201	0.810	-0.070	-0.060
202	0.835	-0.135	-0.050
203	0.893	-0.111	-0.030
204	0.956	-0.124	0.010
205	0.989	-0.111	0.060
206	1.000	-0.075	0.100
207	1.004	-0.021	0.120
208	0.986	0.038	0.110
209	0.978	0.086	0.080
210	0.959	0.118	0.040
211	0.930	0.117	-0.020
212	0.898	0.080	0.070
213	0.900	0.075	0.080
214	0.834	0.023	-0.060
301	0.792	-0.060	-0.080
302	0.834	-0.104	-0.060
303	0.866	-0.111	-0.040
304	0.966	-0.122	0.010
305	1.003	-0.105	0.050
306	1.005	-0.068	0.090
307	1.000	-0.017	0.110
308	0.992	0.037	0.110
309	0.984	0.085	0.080
310	0.968	0.118	0.040
311	0.939	0.123	-0.020
312	0.912	0.086	-0.080
313	0.882	0.064	-0.090
314	0.843	0.019	-0.100

Figure 14 - Wake Velocity Diagram and Test Data, Model 4892

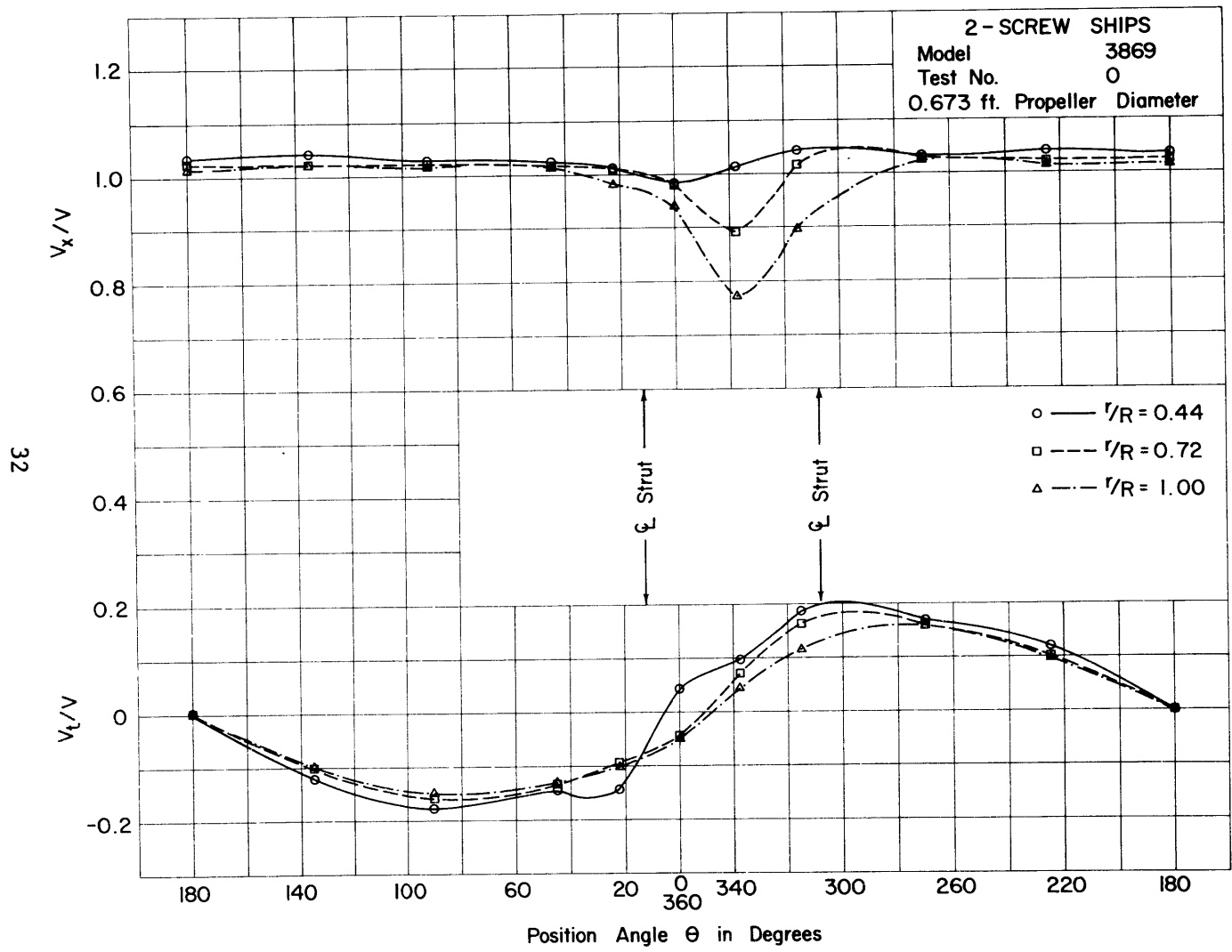


Figure 15 - Circumferential Longitudinal ( $V_x/V$ ) and Tangential ( $V_t/V$ ) Velocity Distributions at Various Test Radii, Model 3869

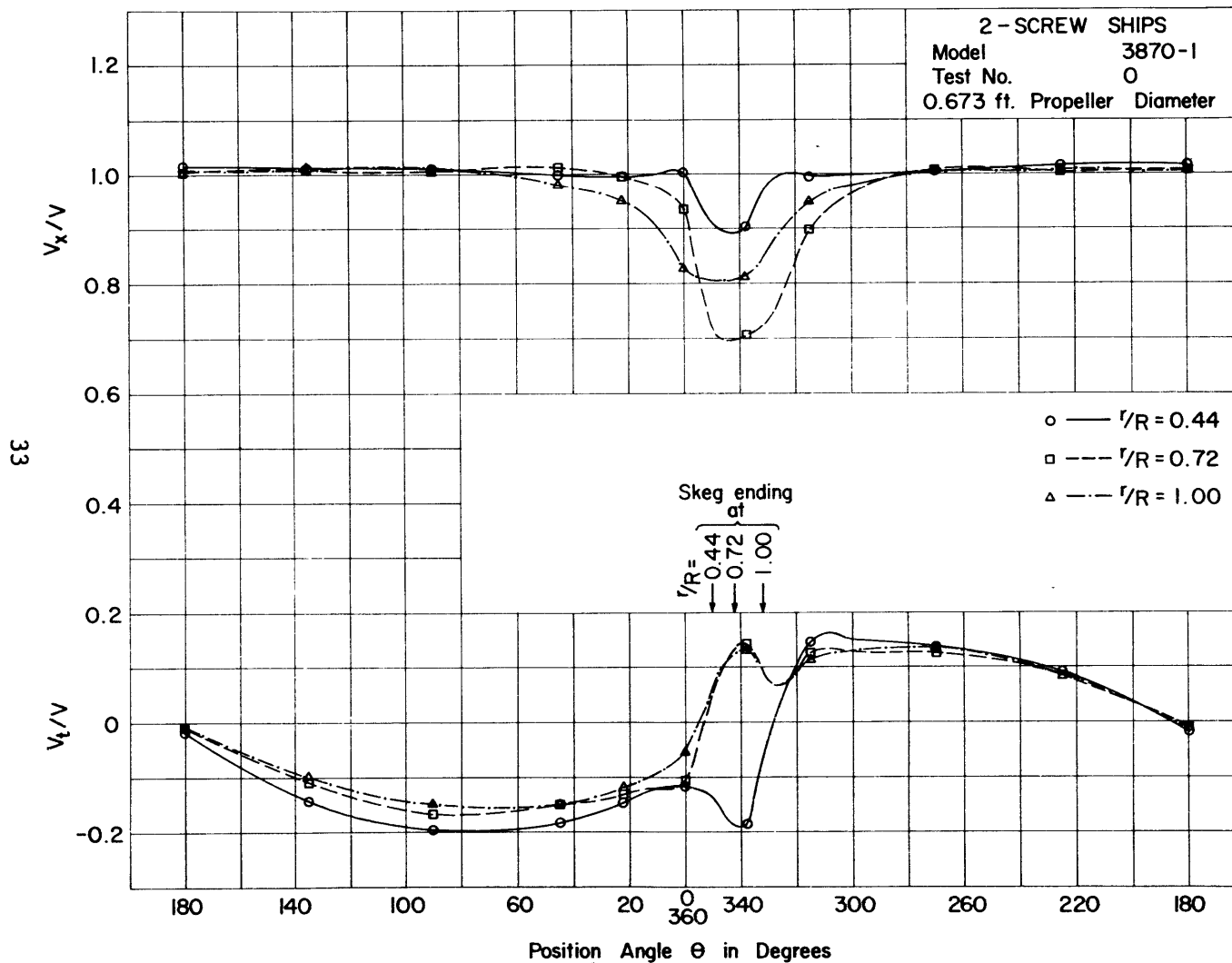


Figure 16 - Circumferential Longitudinal ( $V_x/V$ ) and Tangential ( $V_t/V$ ) Velocity Distributions at Various Test Radii, Model 3870-1

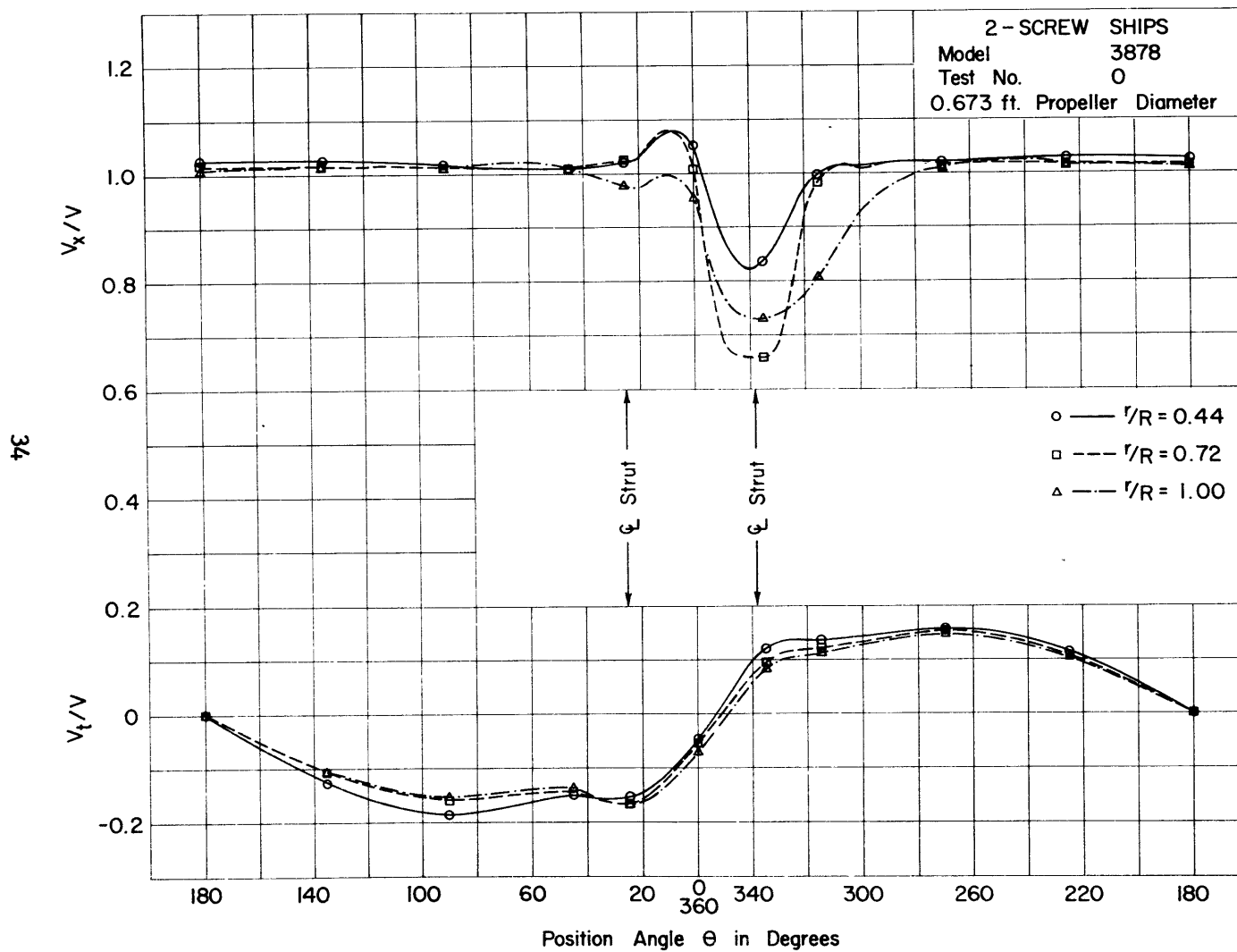


Figure 17 - Circumferential Longitudinal ( $V_x/V$ ) and Tangential ( $V_t/V$ ) Velocity Distributions at Various Test Radii, Model 3878

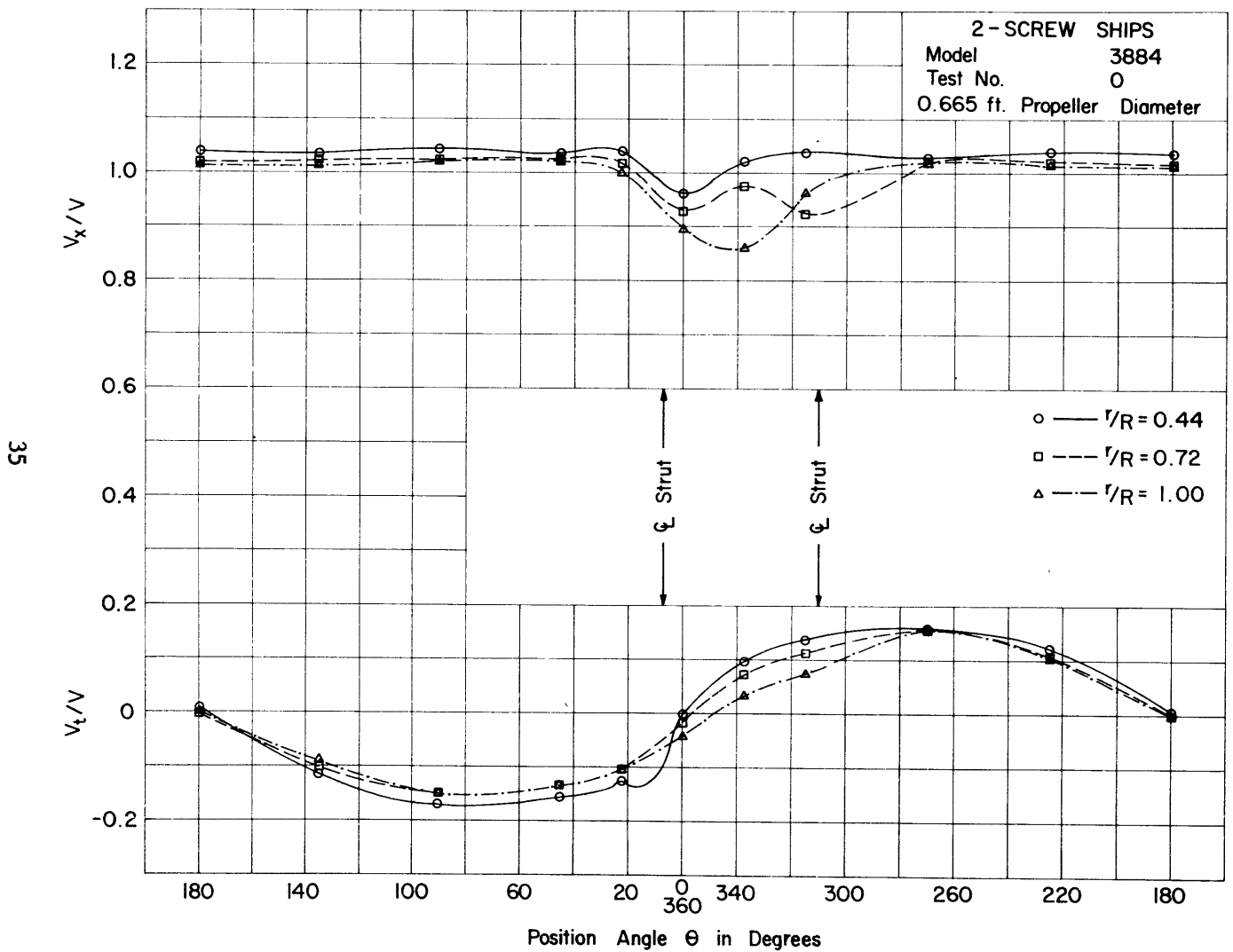


Figure 18 - Circumferential Longitudinal ( $V_x/V$ ) and Tangential ( $V_t/V$ ) Velocity Distributions at Various Test Radii, Model 3884



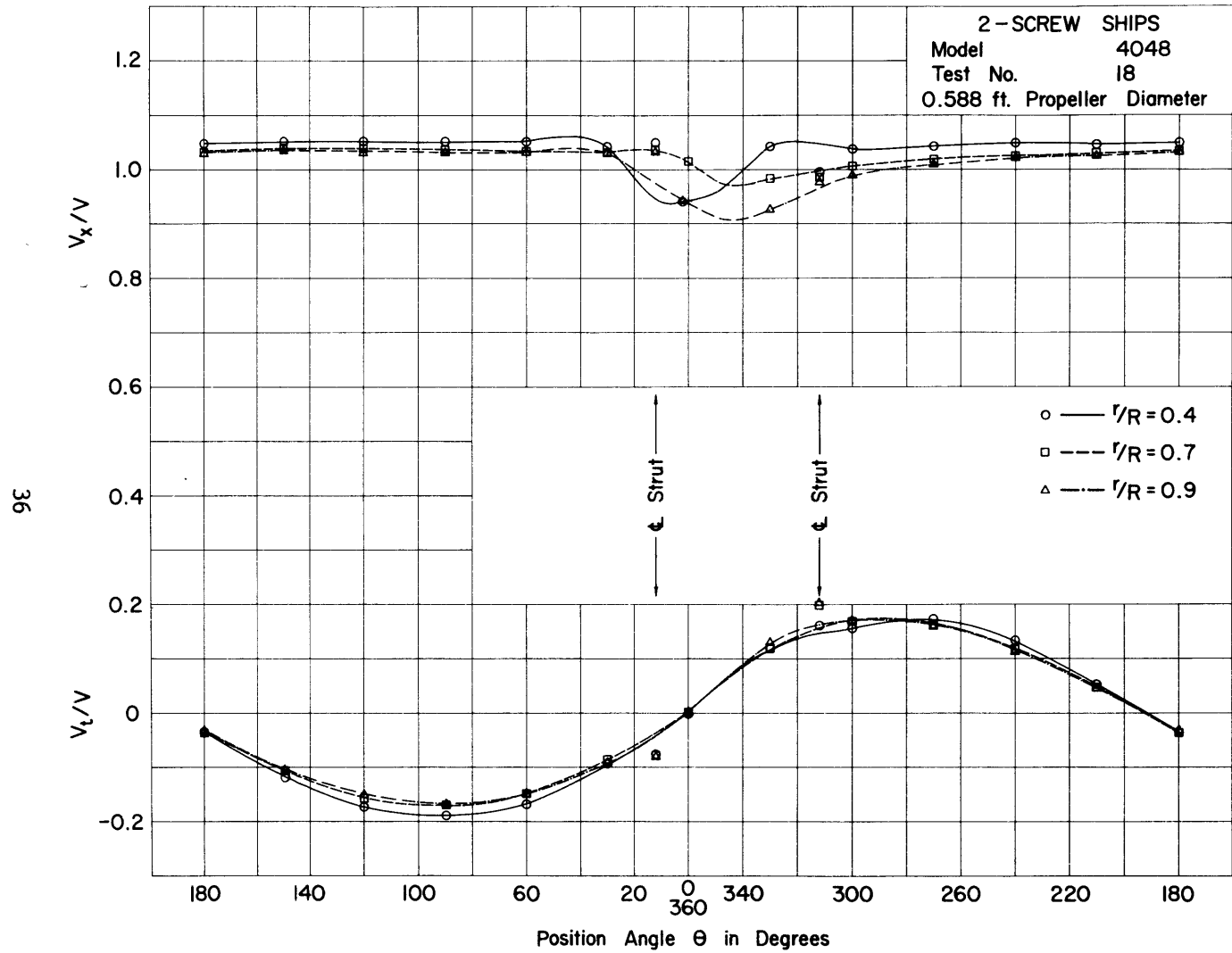


Figure 19 - Circumferential Longitudinal ( $V_x/V$ ) and Tangential ( $V_t/V$ ) Velocity Distributions at Various Test Radii, Model 4048

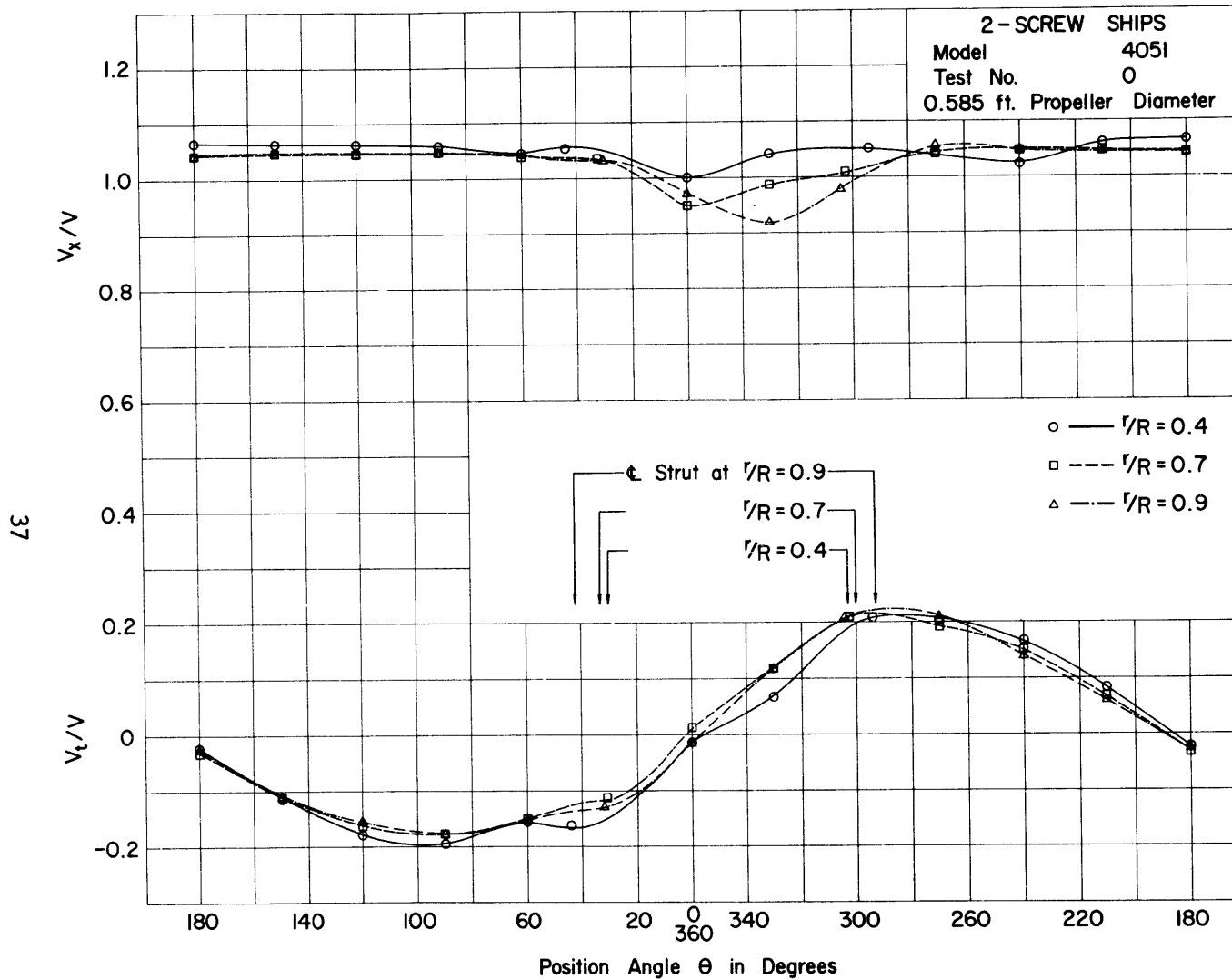


Figure 20 - Circumferential Longitudinal ( $V_x/V$ ) and Tangential ( $V_t/V$ ) Velocity Distributions at Various Test Radii, Model 4051

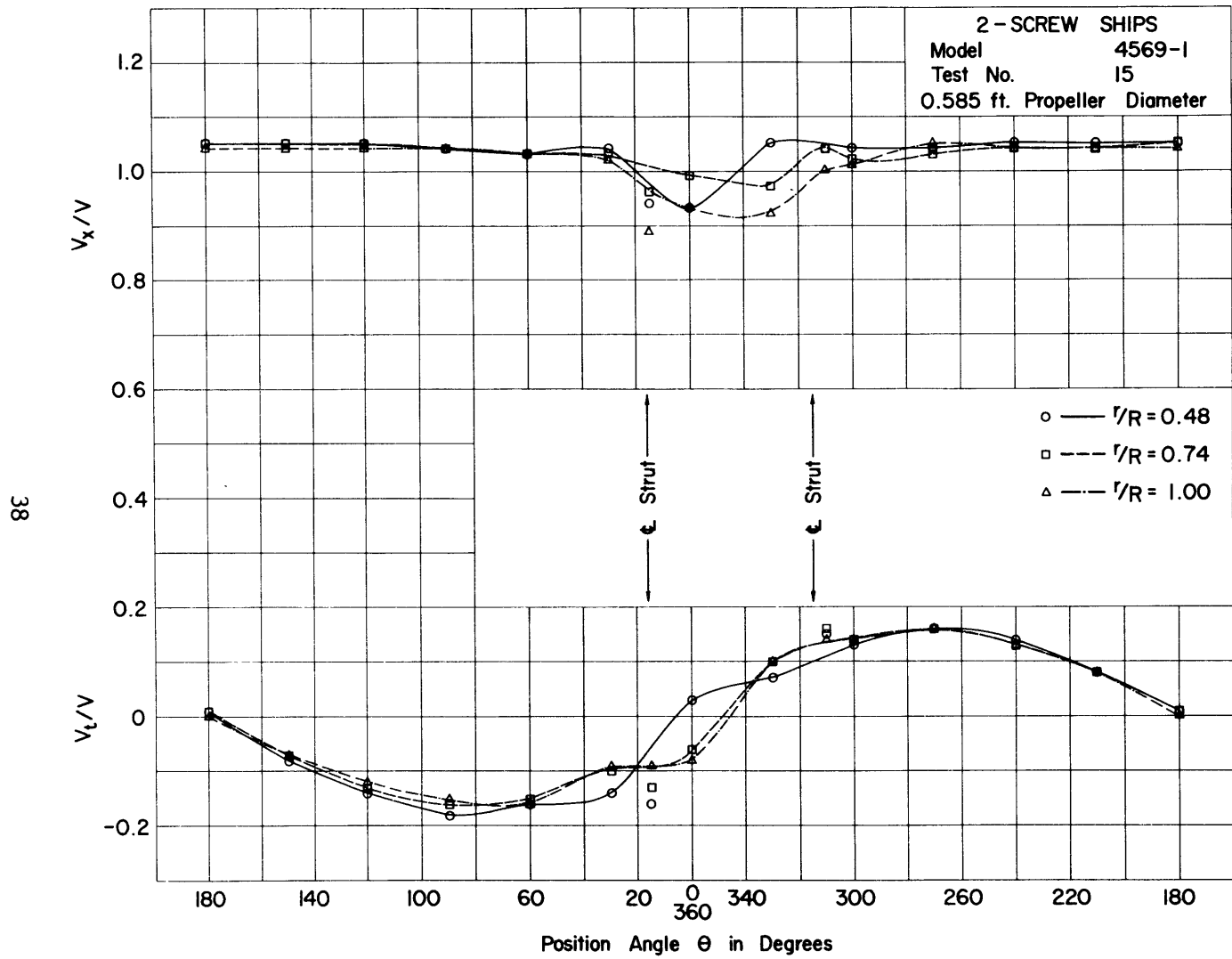


Figure 21 - Circumferential Longitudinal ( $V_x/V$ ) and Tangential ( $V_t/V$ ) Velocity Distributions at Various Test Radii, Model 4569-1

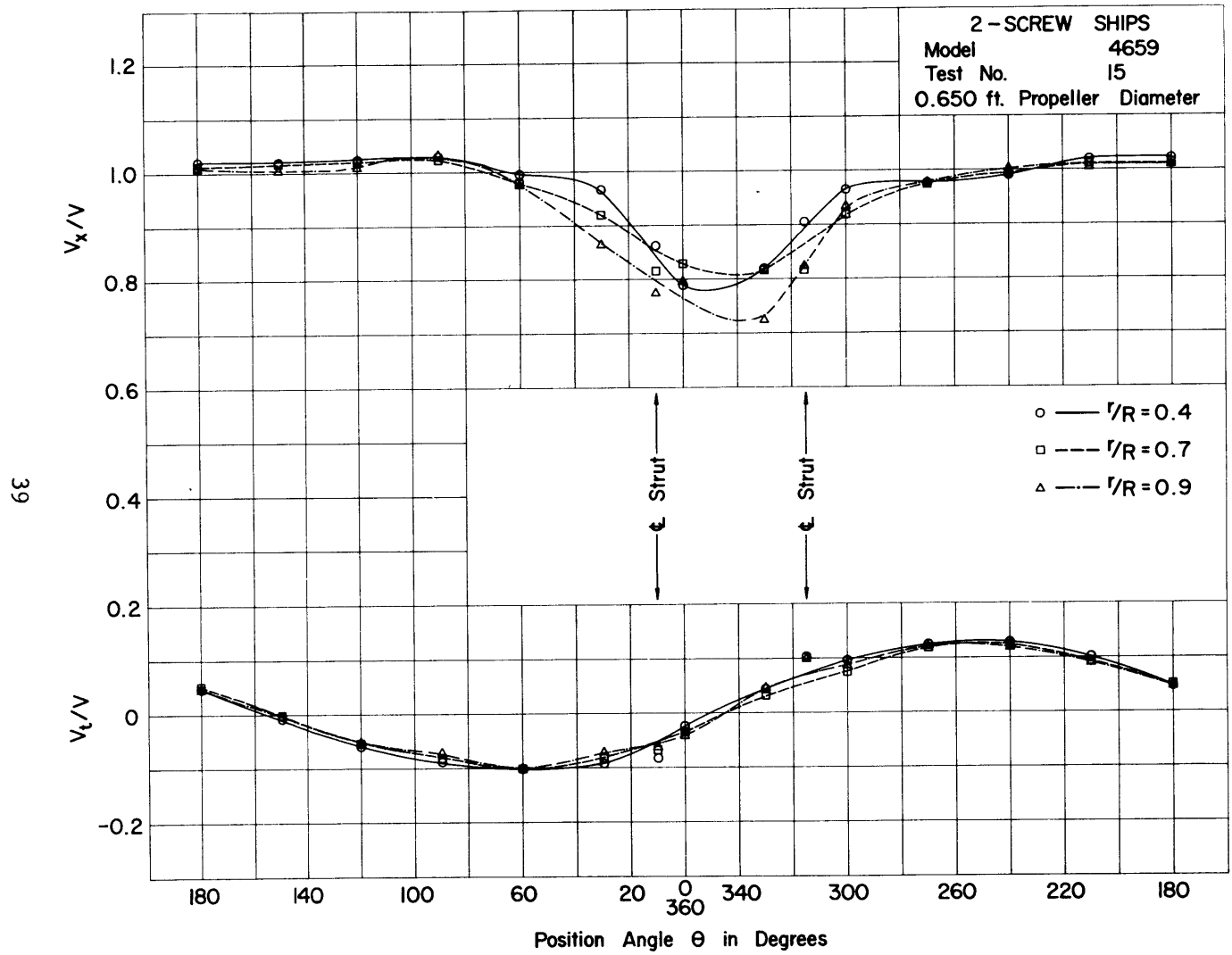


Figure 22 - Circumferential Longitudinal ( $V_x/V$ ) and Tangential ( $V_t/V$ ) Velocity Distributions at Various Test Radii, Model 4659

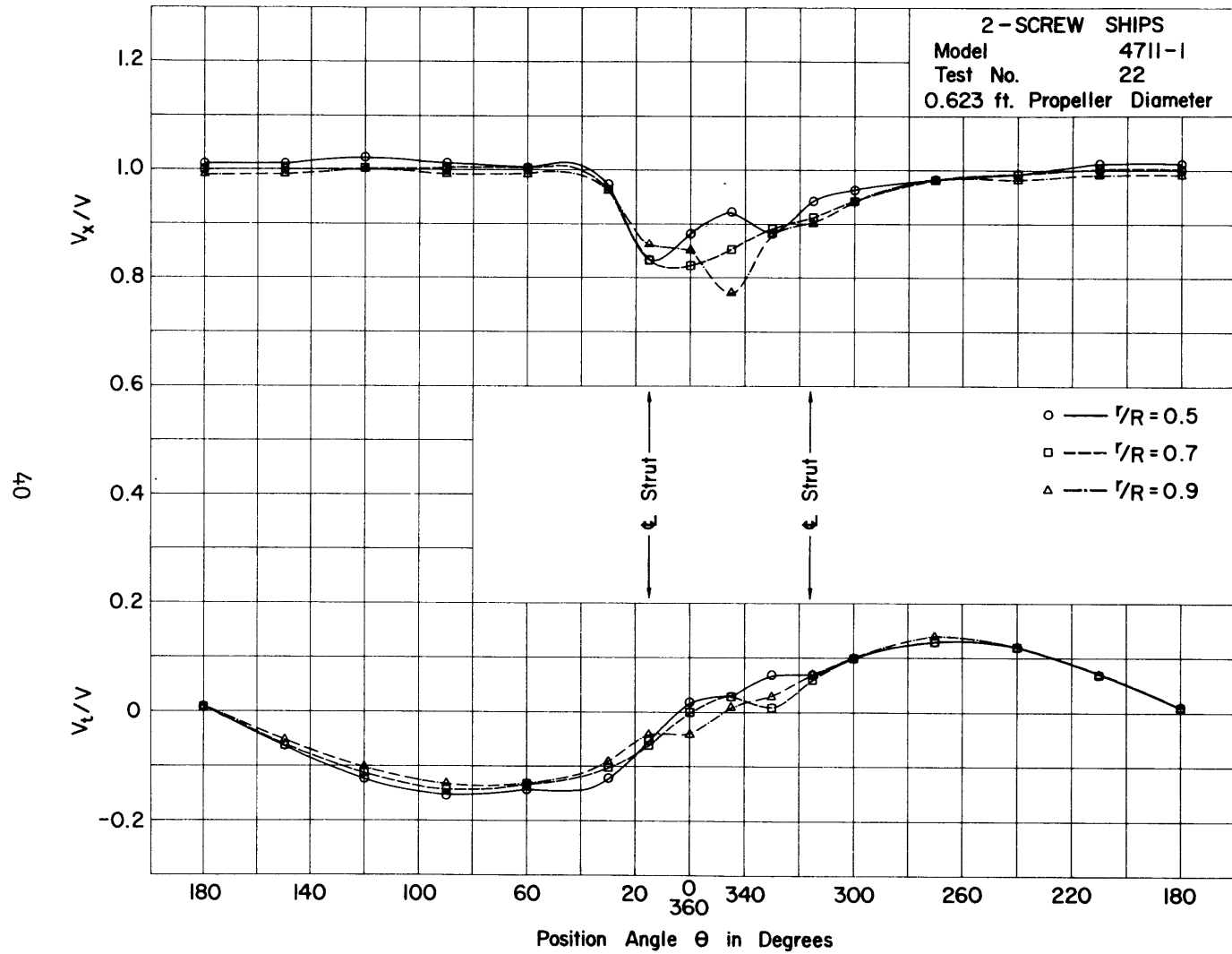


Figure 23 - Circumferential Longitudinal ( $V_x/V$ ) and Tangential ( $V_t/V$ ) Velocity Distributions at Various Test Radii, Model 4711-1

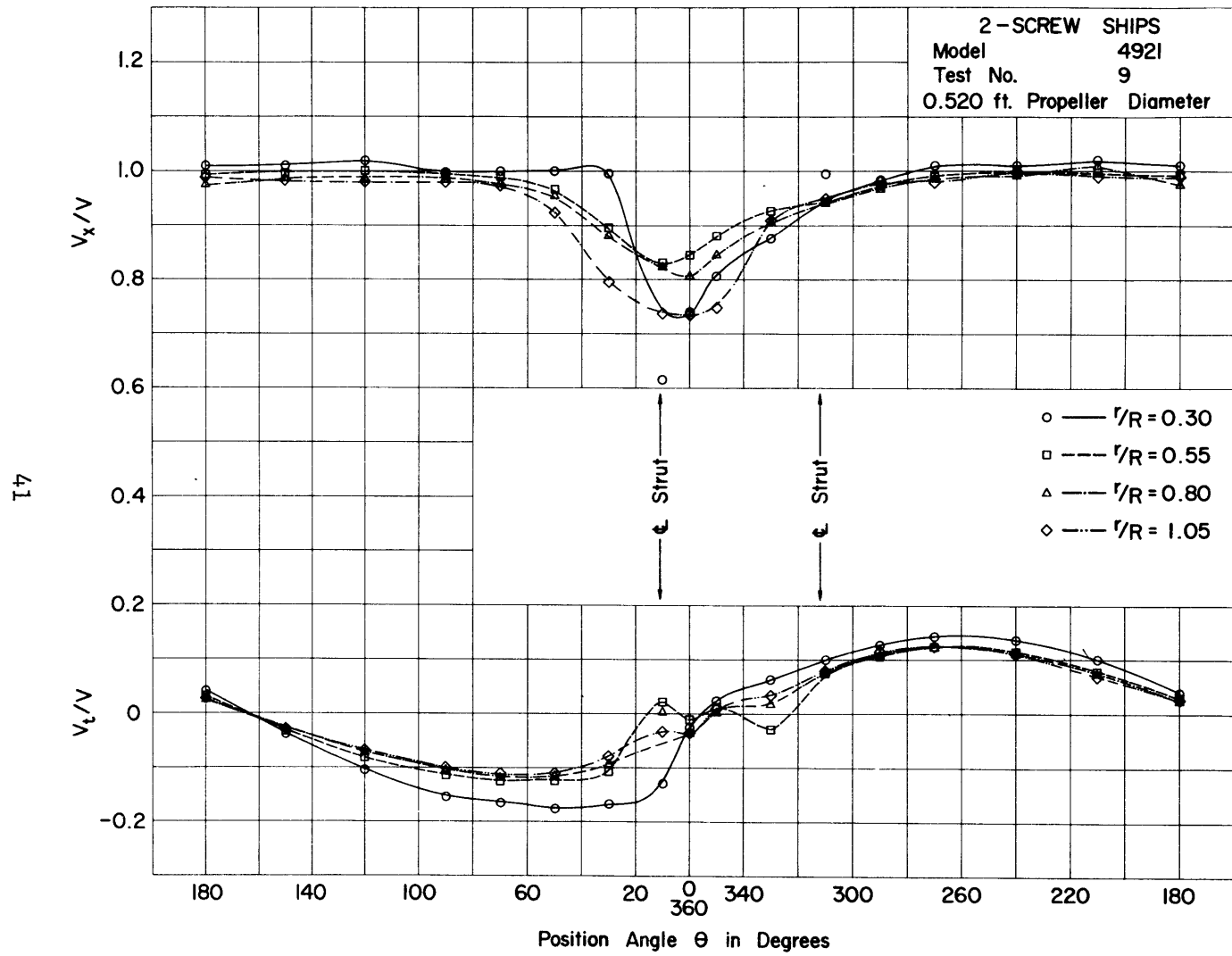


Figure 24 - Circumferential Longitudinal ( $V_x/V$ ) and Tangential ( $V_t/V$ ) Velocity Distributions at Various Test Radii, Model 4921

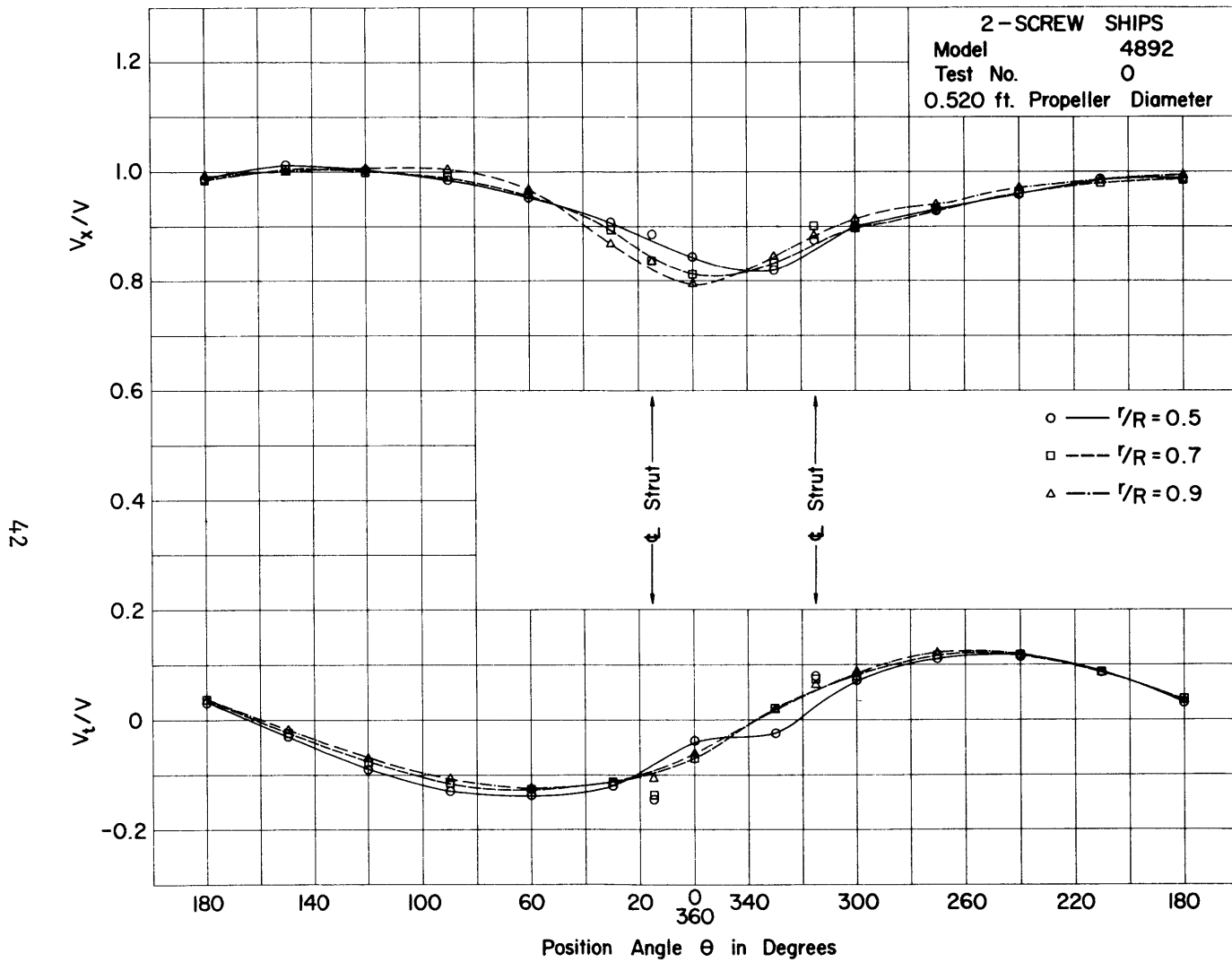


Figure 25 - Circumferential Longitudinal ( $V_x/V$ ) and Tangential ( $V_t/V$ ) Velocity Distributions at Various Test Radii, Model 4892

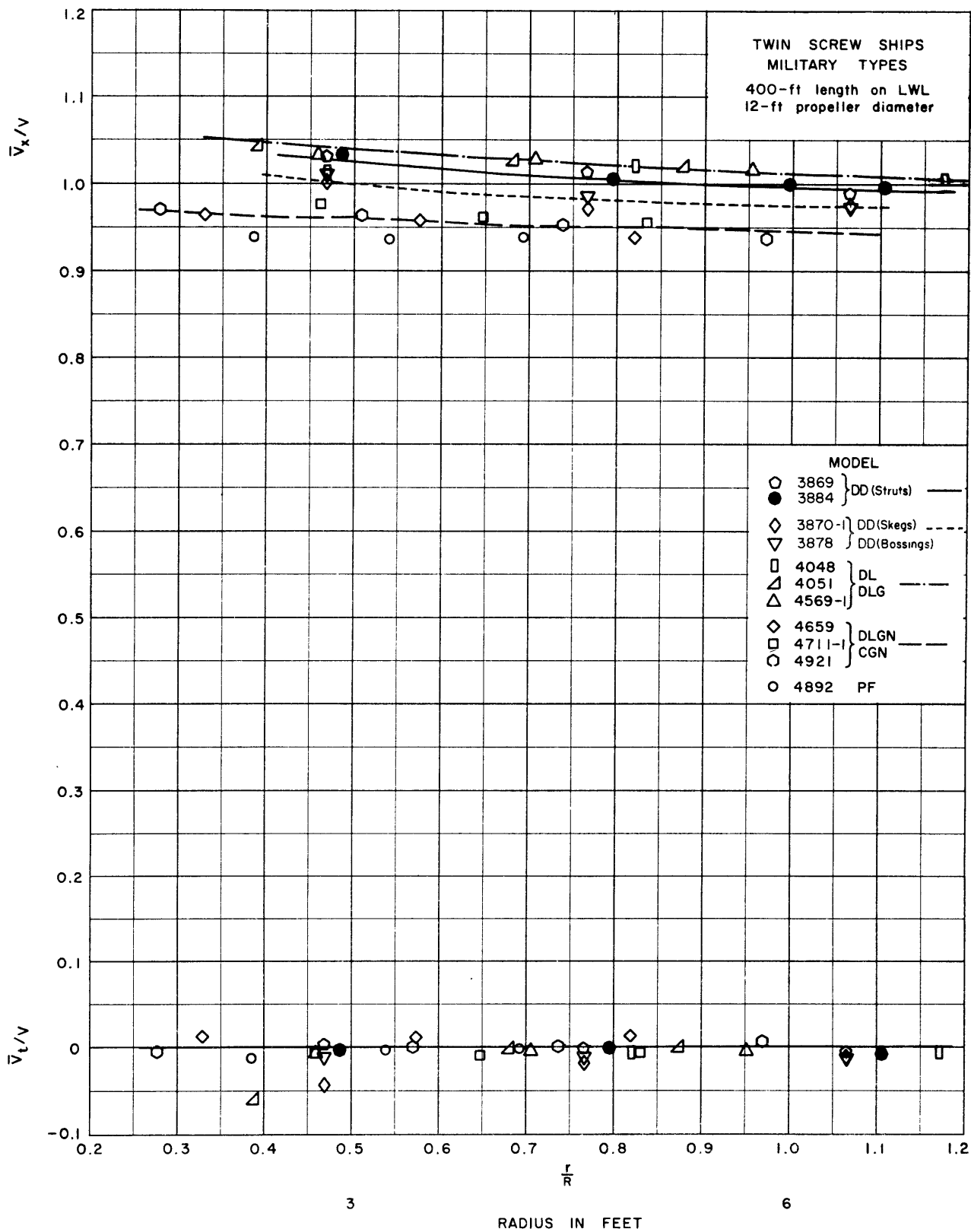


Figure 26 - Mean Longitudinal Velocity ( $\bar{V}_x/V$ ) and Mean Tangential Velocity ( $\bar{V}_t/V$ )



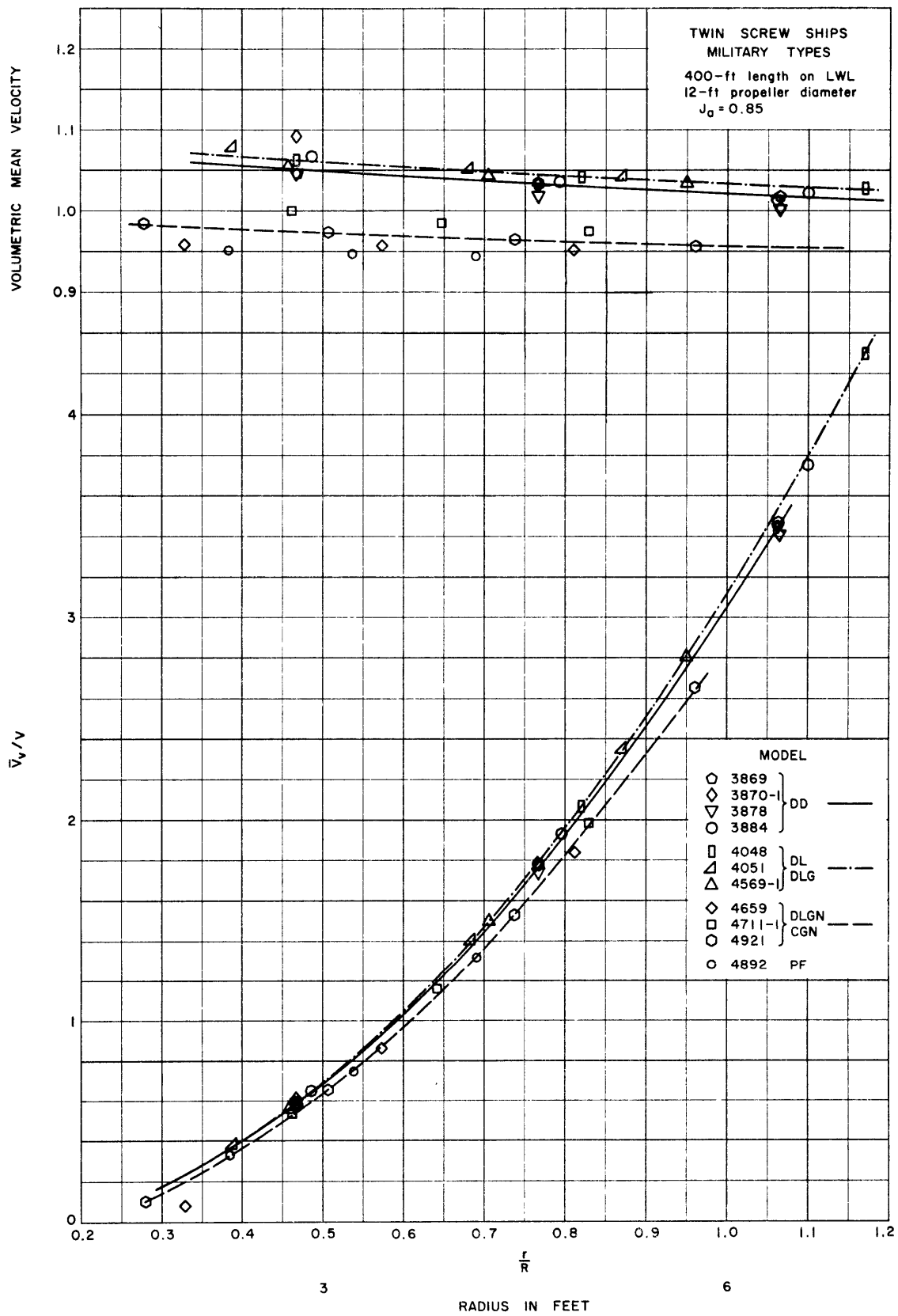


Figure 27 - Calculated Volumetric Velocity ( $\bar{V}_v/V$ ) and Volumetric Mean Velocity

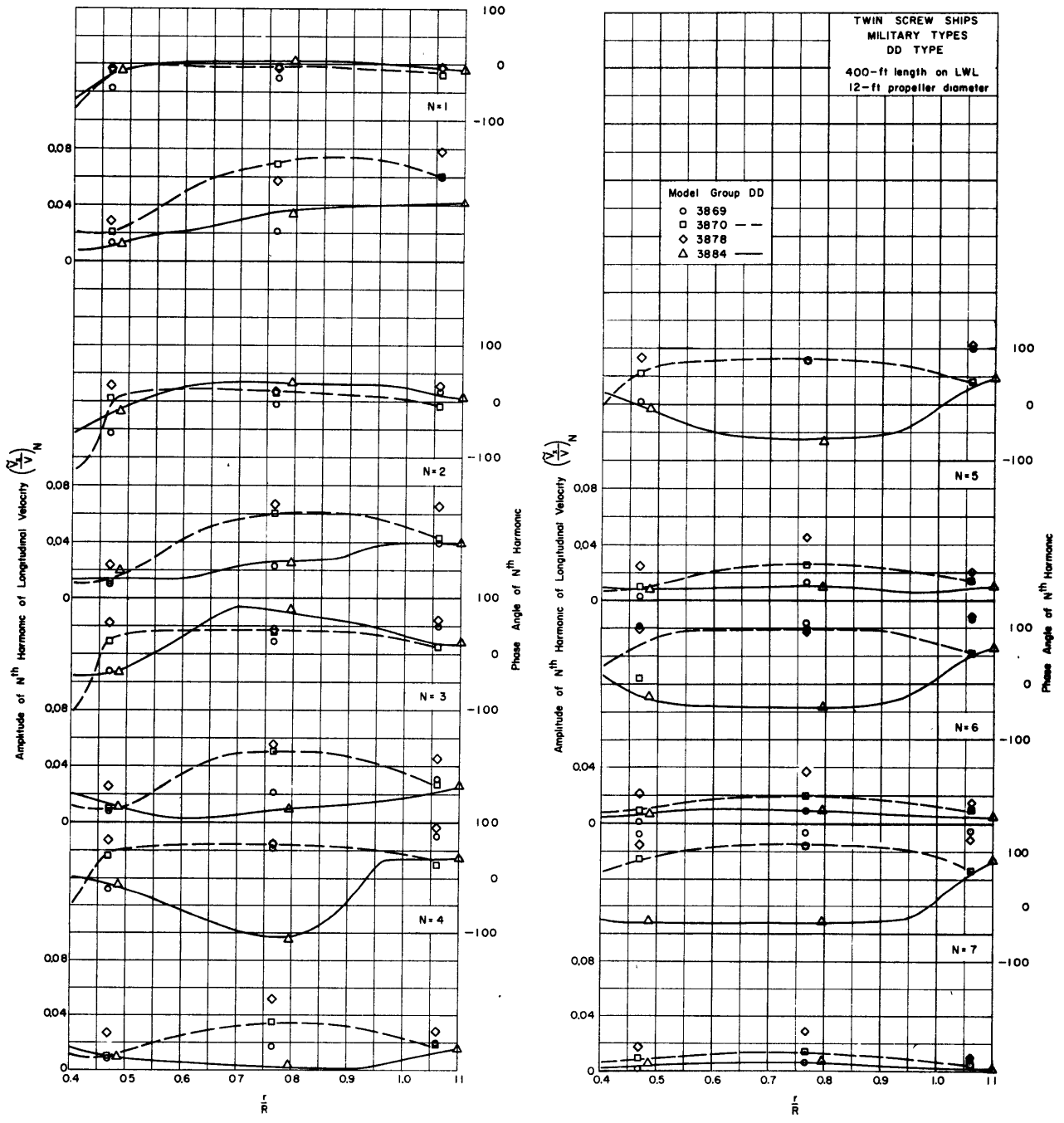


Figure 28 - Amplitudes and Phase Angles of Various Harmonics of Longitudinal  $(\tilde{V}_x/V)$  Velocity Components, DD Type

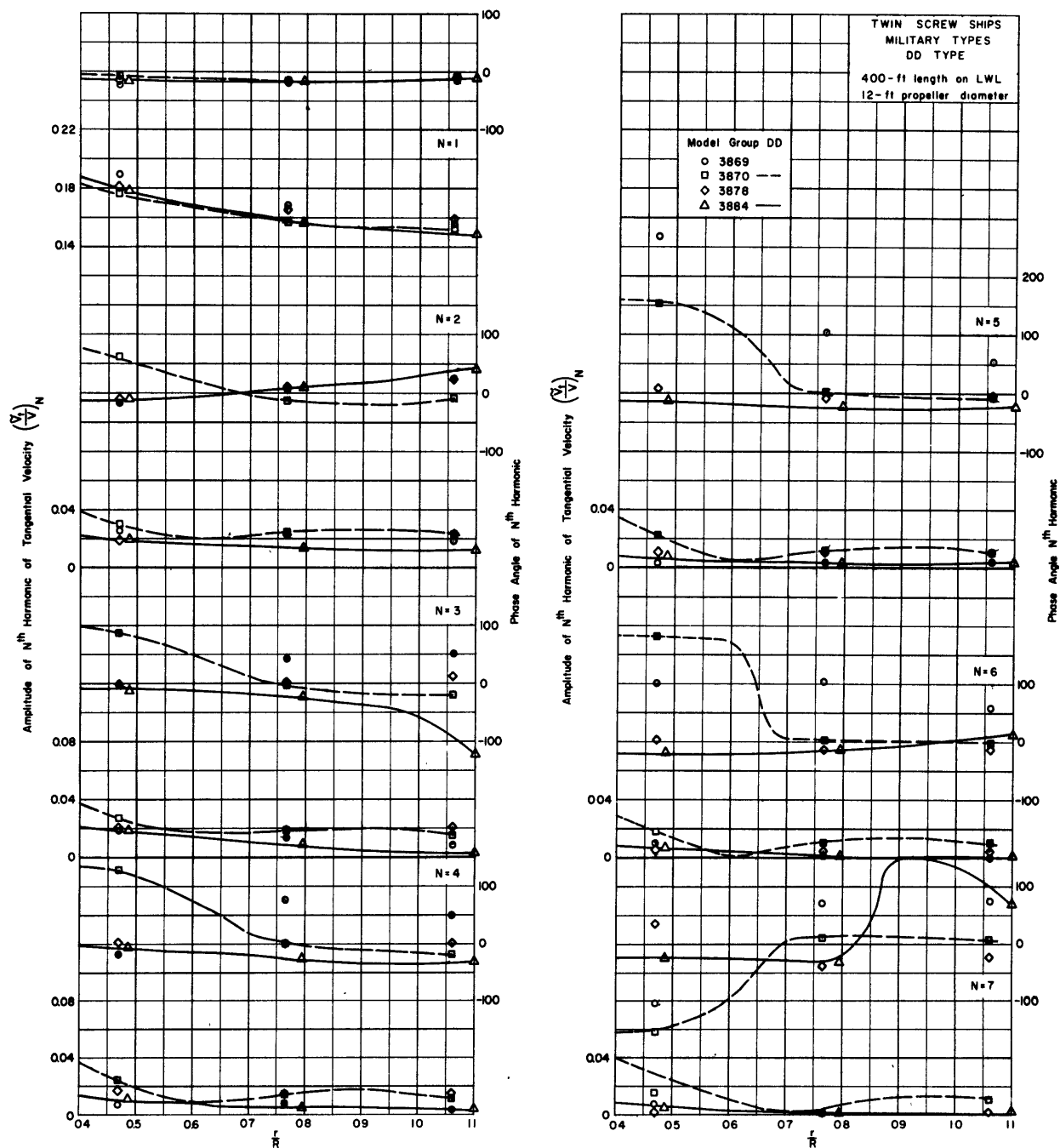


Figure 29 - Amplitude and Phase Angle of Various Harmonics of Tangential  $(\bar{V}_t/V)$  Velocity Components, DD Type

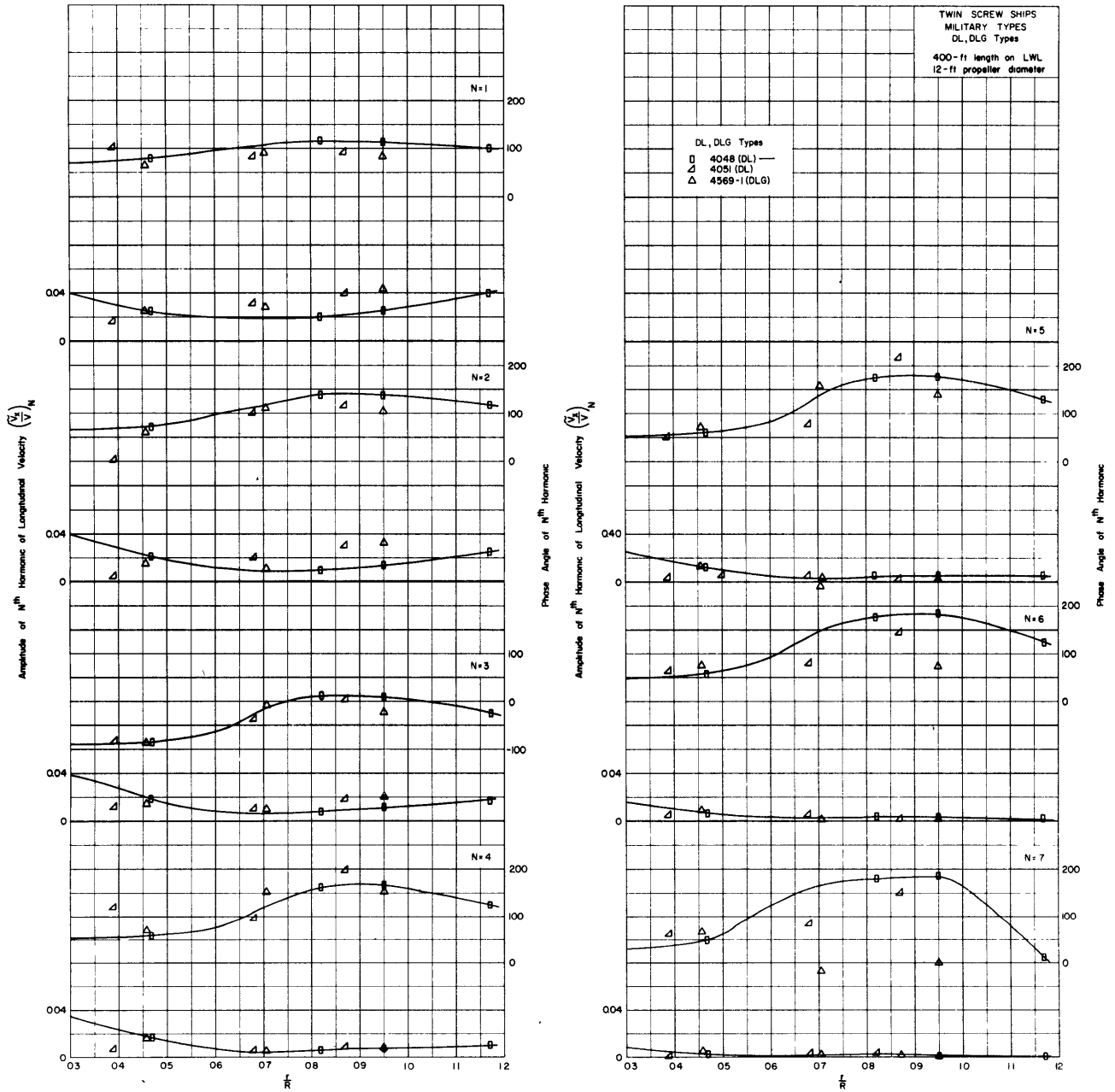


Figure 30 - Amplitude and Phase Angles of Various Harmonics of Longitudinal  $\left(\frac{\tilde{V}_x}{V}\right)$  Velocity Components, DL and DLG Types

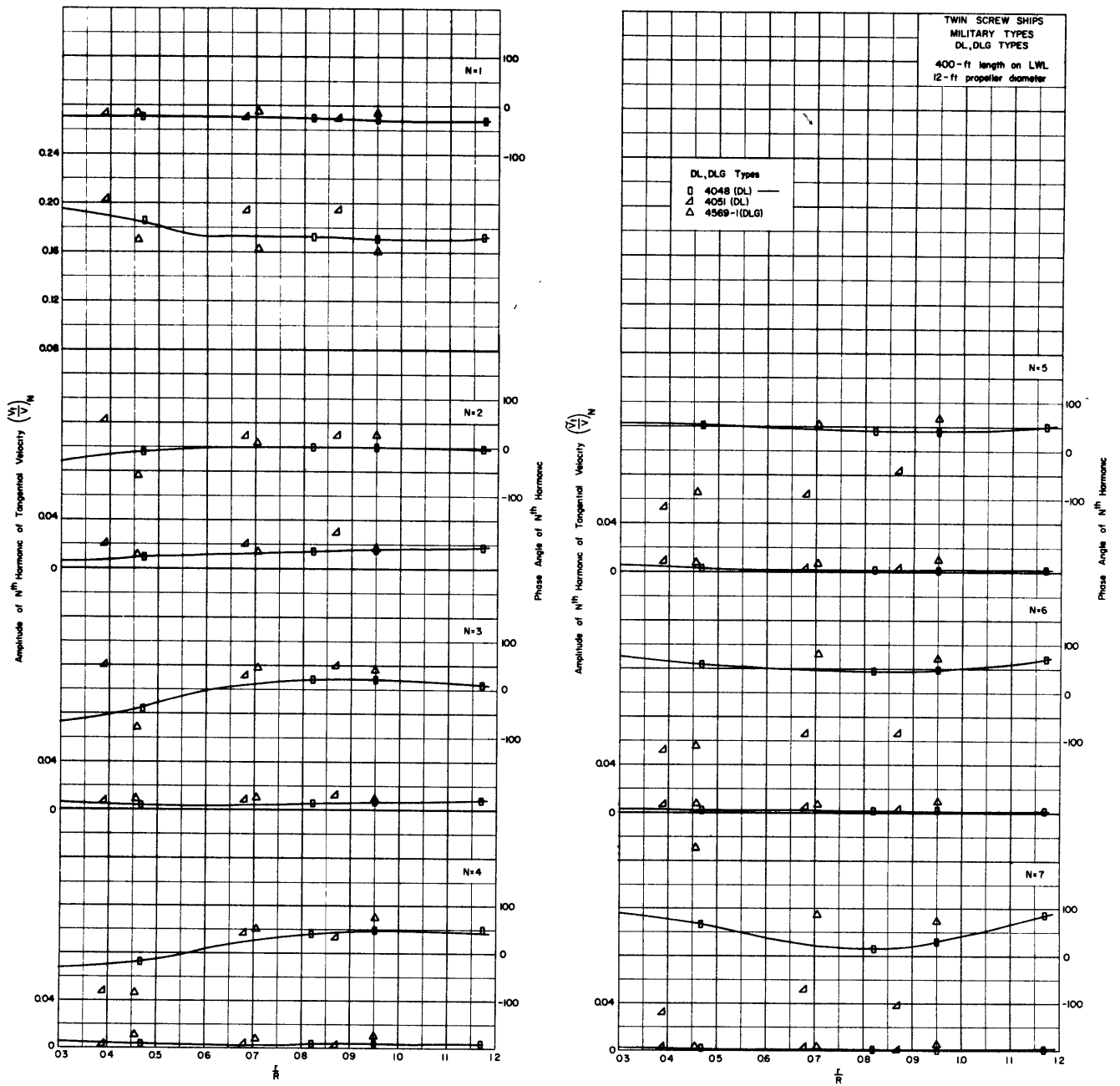


Figure 31 - Amplitude and Phase Angles of Various Harmonics of Tangential  $\left(\vec{V}_t/V\right)$  Velocity Components, DL and DLG Types

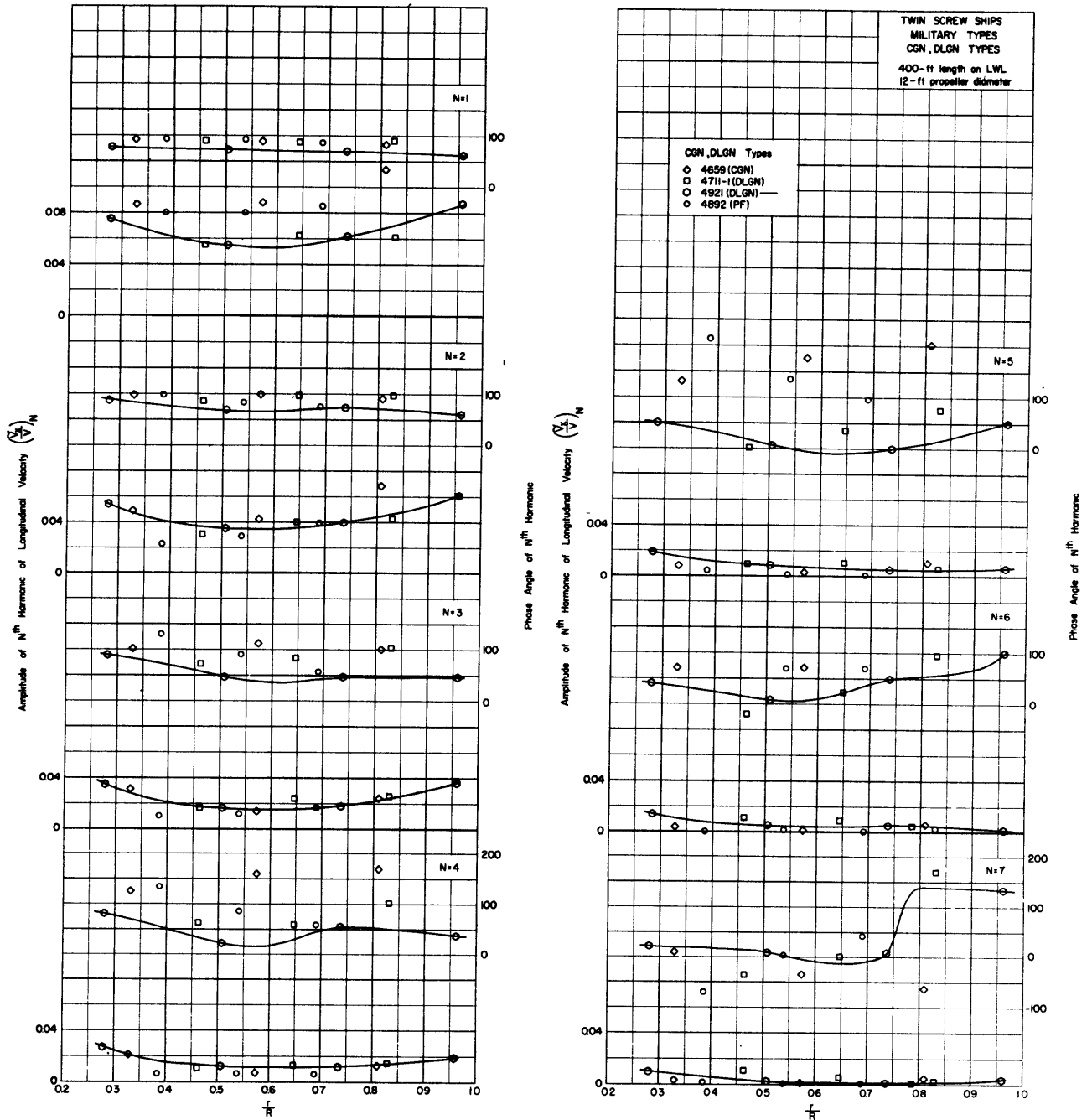


Figure 32 - Amplitude and Phase Angles of Various Harmonics of Longitudinal  $(\frac{V_x}{V})$  Velocity Components, CGN and DLGN Types

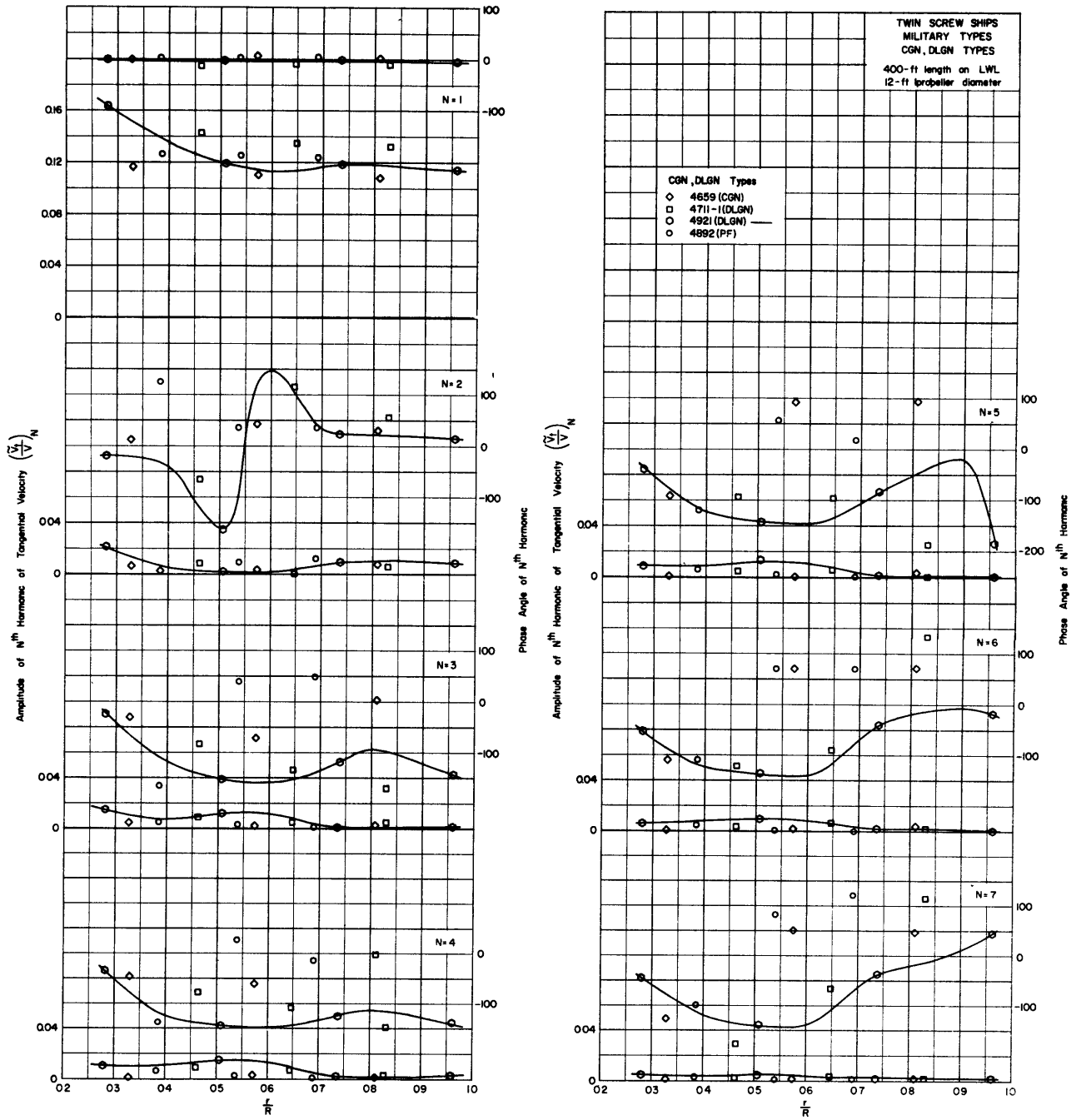


Figure 33 - Amplitude and Phase Angles of Various Harmonics of Tangential ( $\tilde{V}_t/V$ ) Velocity Components, CGN and DLGN Types

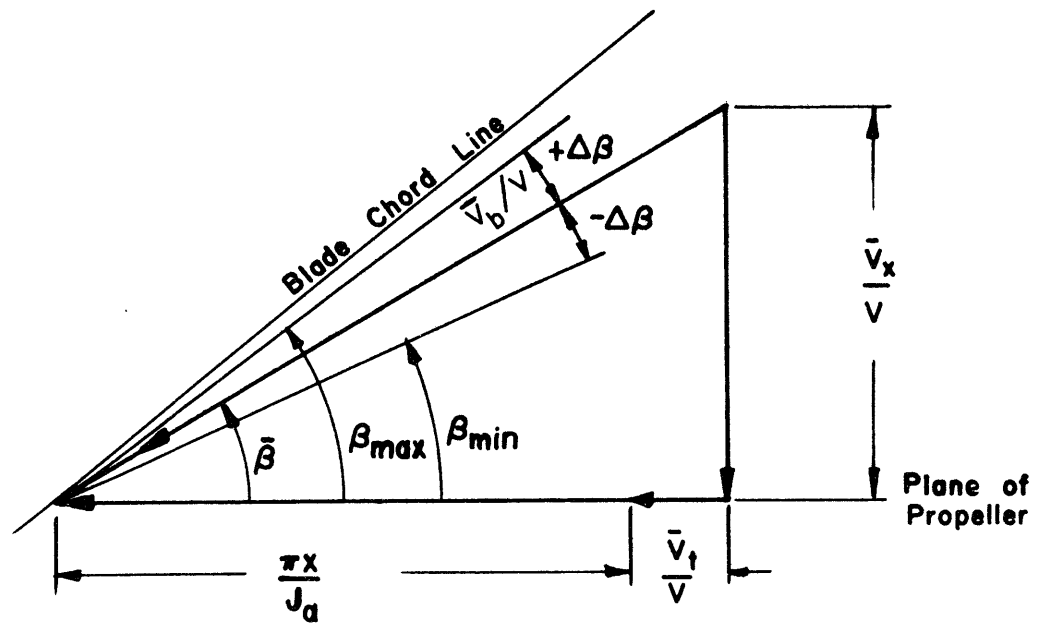


Figure 34 - Velocity Diagram



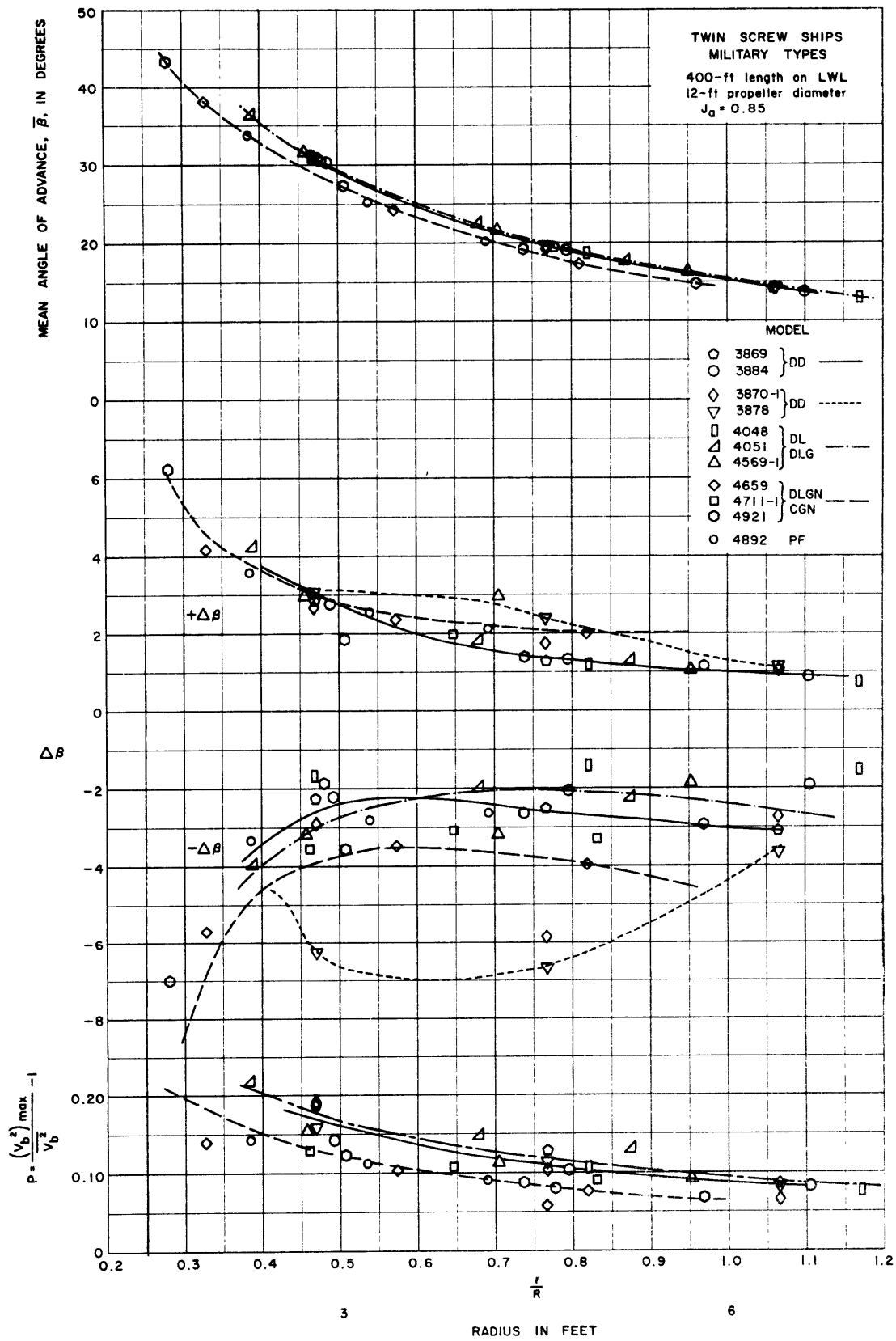


Figure 35 - Mean Advance Angles ( $\bar{\beta}$ ), Variations in Beta Angles ( $\Delta\beta$ ) And Pressure Factor (P)

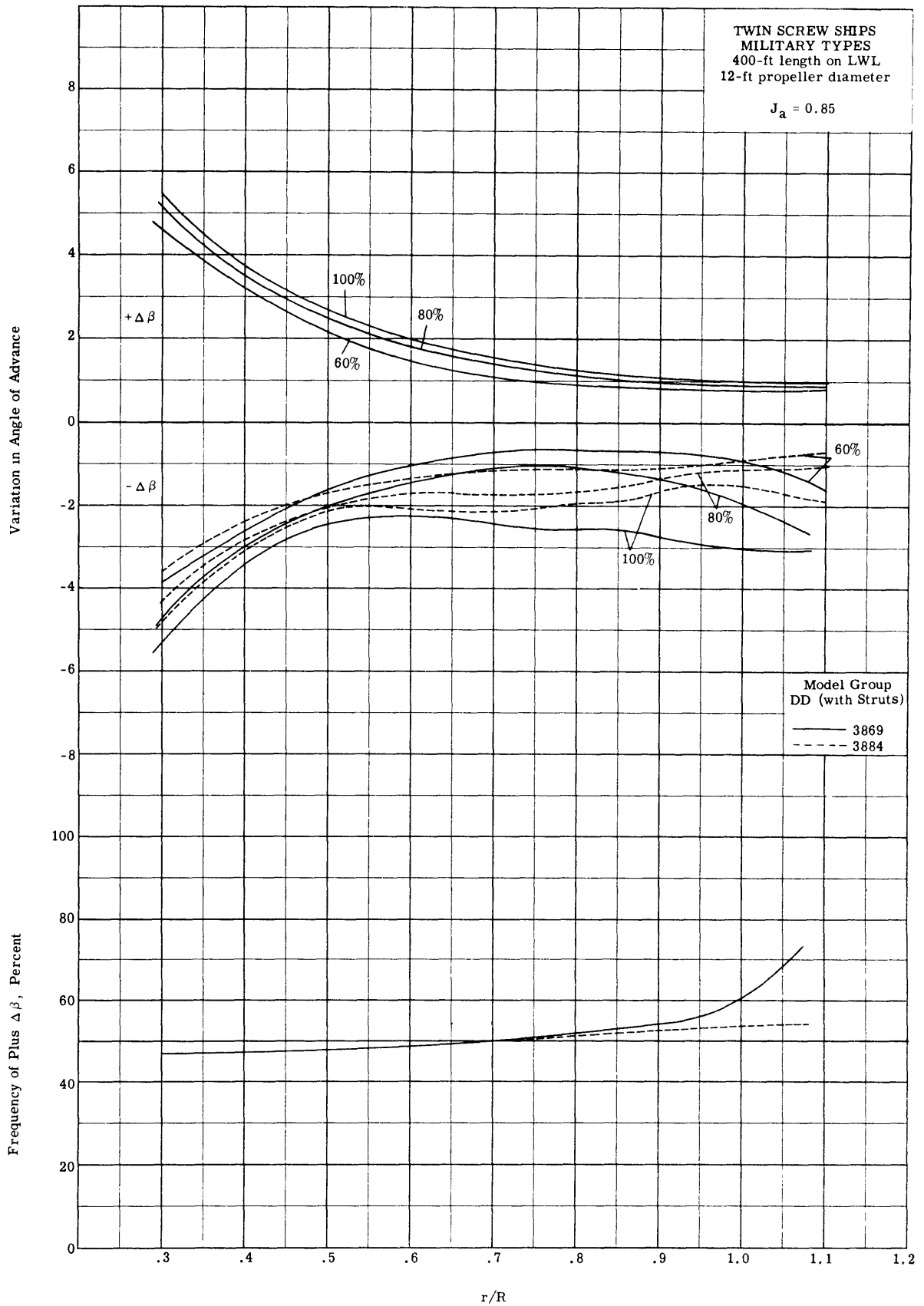


Figure 36 - Variations in Angle of Advance and Frequency of Plus  $\Delta\beta$ , DD Type (with Struts)

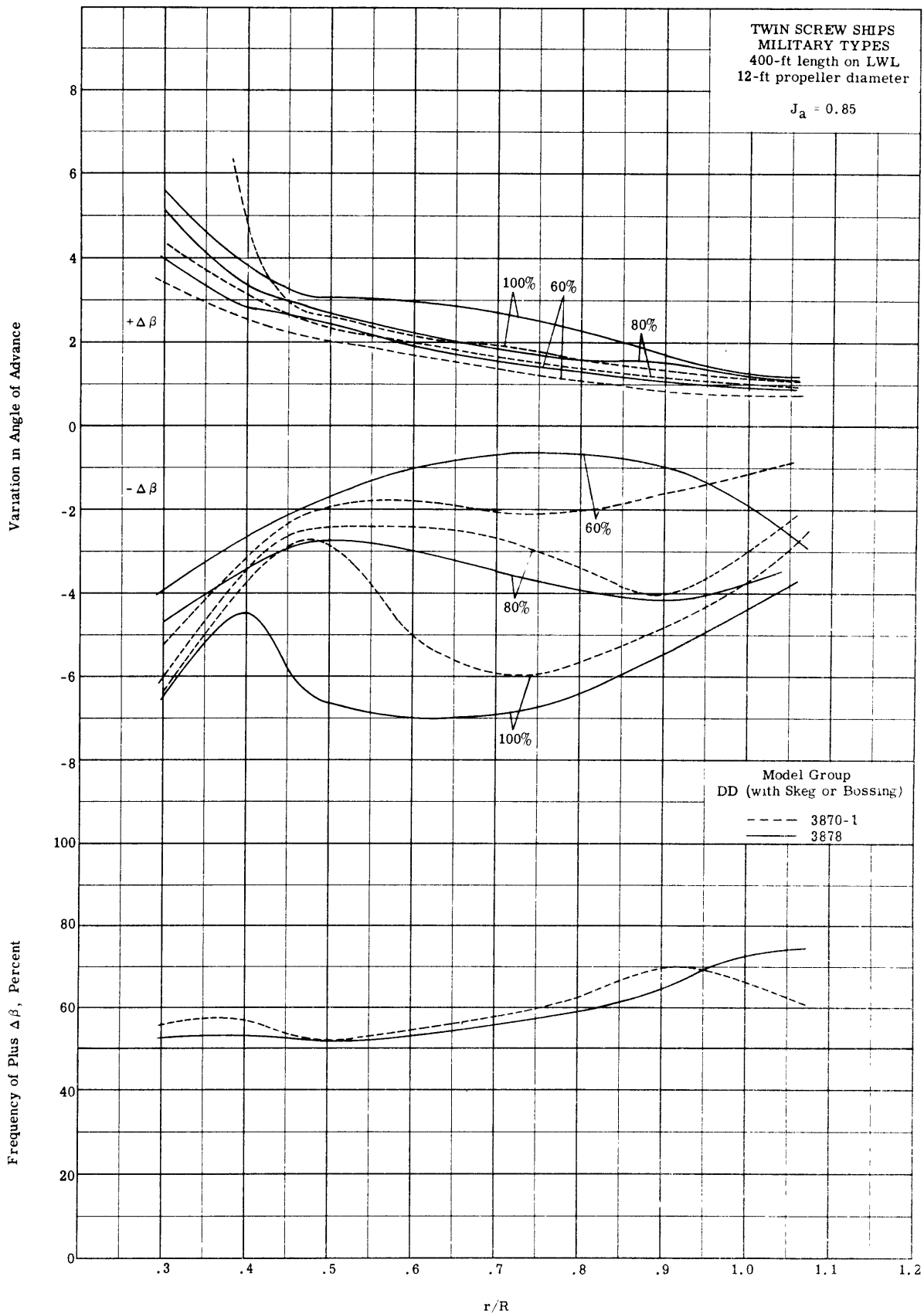


Figure 37 - Variation in Angle of Advance and Frequency of Plus  $\Delta\beta$ , DD Type (with Skeg or Bossing)

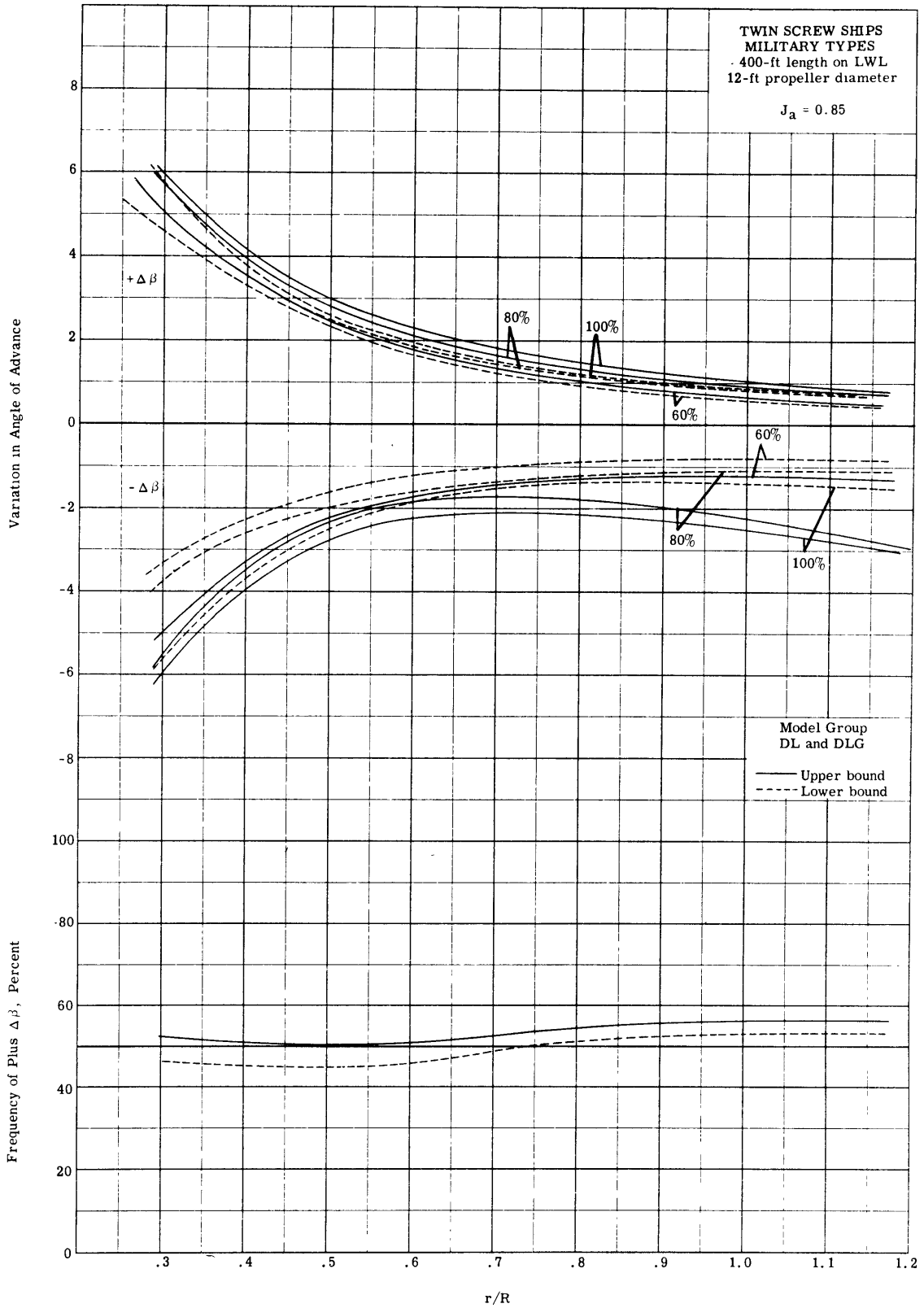


Figure 38 - Variation in Angle of Advance and Frequency of Plus  $\Delta\beta$ , DL and DLG Types

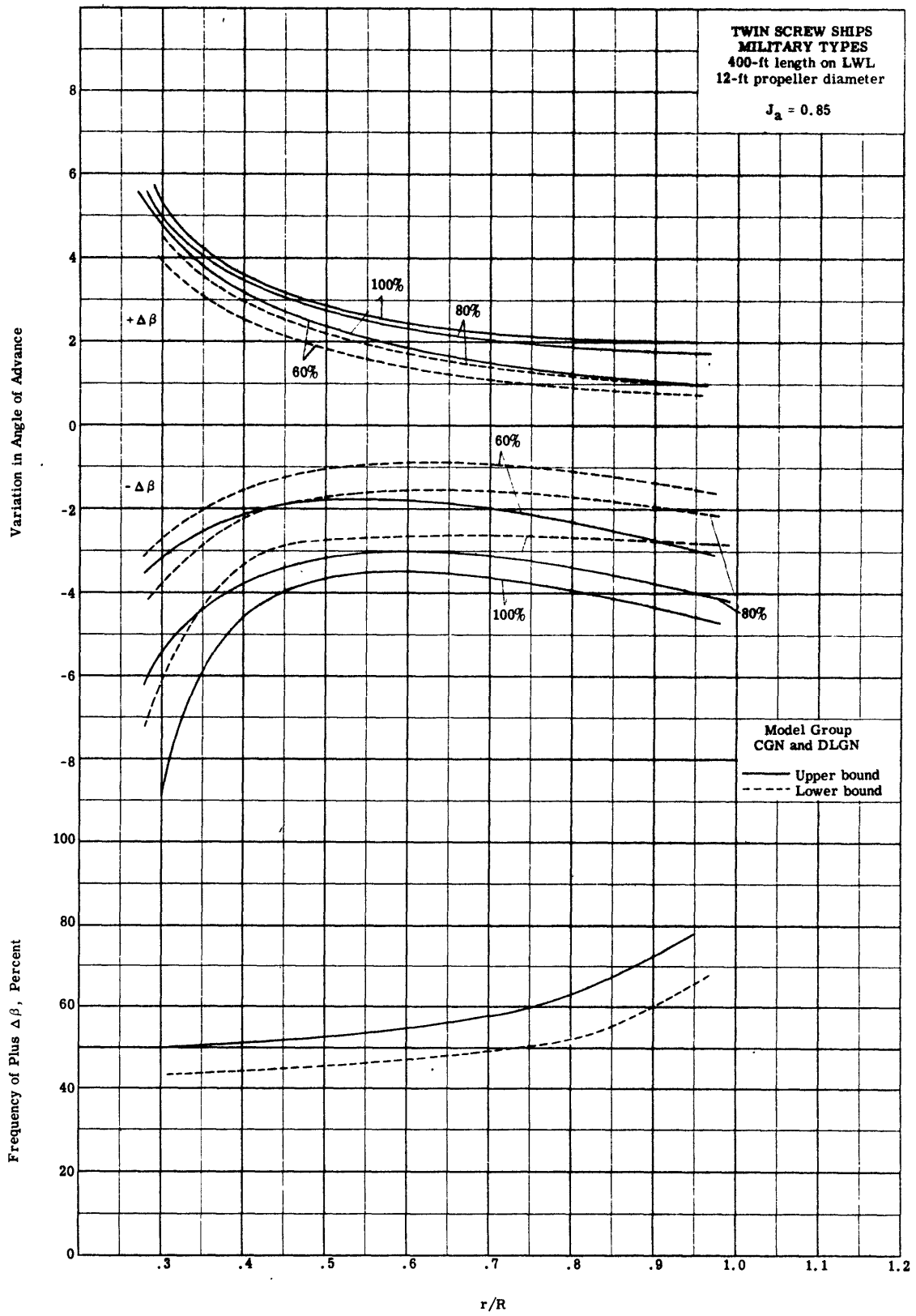


Figure 39 - Variation in Angle of Advance and Frequency of Plus  $\Delta\beta$ , CGN and DLGN Types

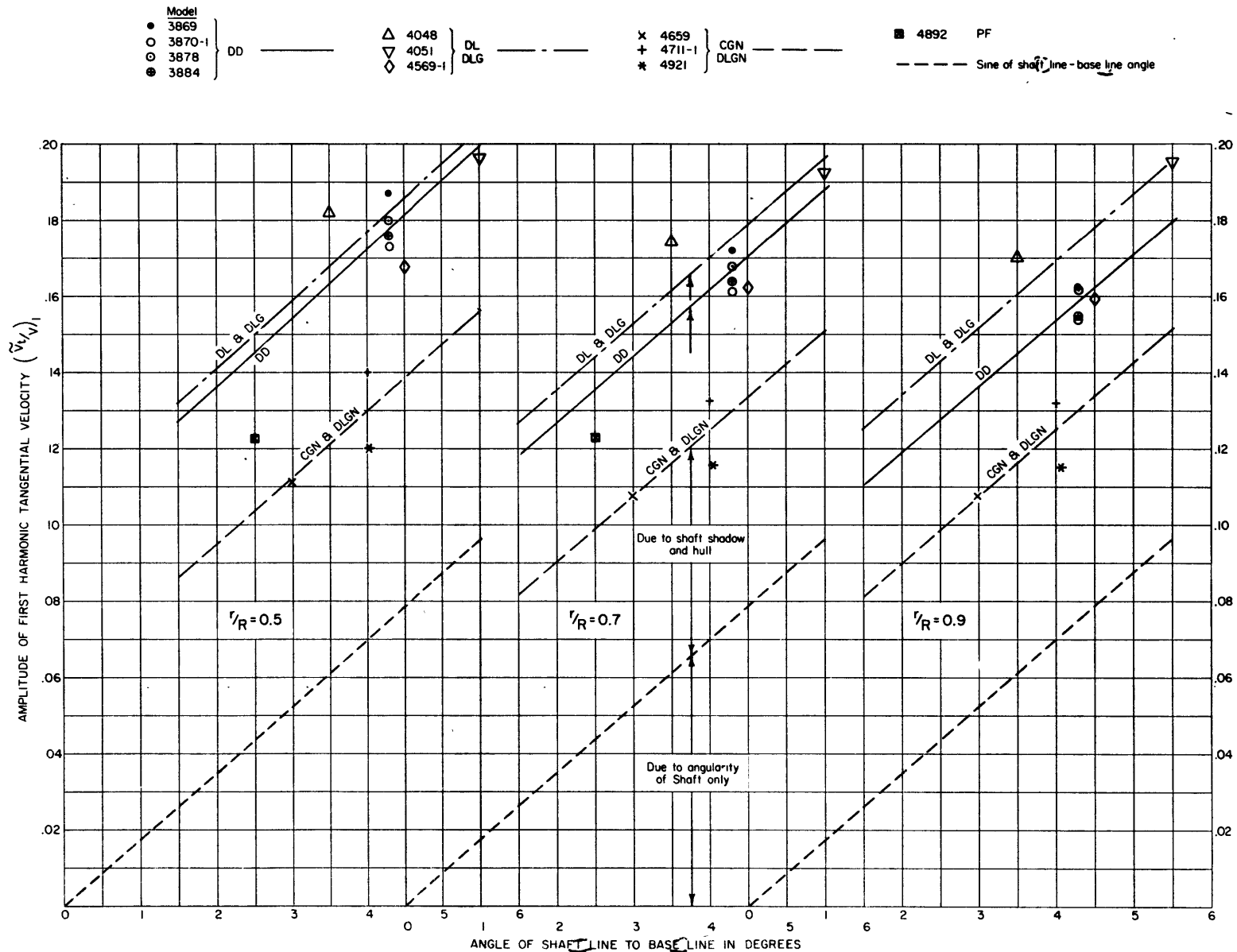


Figure 40 - Amplitude of First Harmonic of Tangential Velocity  $(\tilde{v}_t/V)_1$  versus Angle of Shaftline to Baseline

INITIAL DISTRIBUTION

Copies

13 CHBUSHIPS  
3 Tech Lib (Code 210-L)  
1 Appl Res (Code 340)  
1 Prelim Des (Code 420)  
1 Mach Sci & Res (Code 436)  
1 Hull Des (Code 440)  
1 Prop Shaft & Brng (Code 644)  
1 Lab Mgt (Code 320)  
1 Ship Silencing Br (Code 345)  
1 Cruisers and Destroyers Br (Code 523)  
2 Sci & Res (Code 442)

1 CHBUWEPS  
1 Library (DLI-3)

3 CHONR  
2 Fluid Dyn Br (Code 438)  
1 Library (Code 740)

1 SUPT, USNAVPGSCOL  
1 DIR, ORL  
1 ADMIN, Maritime Admin  
20 DDC  
1 SNAME  
1 HD, NAME, MIT  
1 DIR, Iowa Inst. of Hydraulic Res  
1 DIR, St. Anthony Falls Hydraulic Lab  
1 HD, Dept NAME, Univ of Mich  
1 ADMIN, Inst NAVARCH, Webb  
1 DIR, Inst. of Eng Res, Univ of Calif  
1 DIR, Hydronautics, Inc.

UNCLASSIFIED

Security Classification

DOCUMENT CONTROL DATA - R&D		
<i>(Security classification of title, body of abstract and indexing annotation must be entered when the overall report is classified)</i>		
1 ORIGINATING ACTIVITY (Corporate author)		2a REPORT SECURITY CLASSIFICATION
David Taylor Model Basin, Dept of Navy, Washington, D.C., 20007		UNCLASSIFIED
		2b GROUP
3 REPORT TITLE		
WAKE ANALYSIS OF SHIP MODELS TWIN-SCREW MILITARY TYPES		
4 DESCRIPTIVE NOTES (Type of report and inclusive dates)		
Second of Series		
5 AUTHOR(S) (Last name, first name, initial)		
Cheng, H. M. Hadler, J. B.		
6 REPORT DATE	7a. TOTAL NO. OF PAGES	7b NO OF REFS
December 1964	66	6
8a CONTRACT OR GRANT NO.		9a ORIGINATOR'S REPORT NUMBER(S)
b. PROJECT NO Subproject S-R011-0101		DTMB Report 1928
c Task 0401		9b OTHER REPORT NO(S) (Any other numbers that may be assigned this report)
d		DTMB Report 1849
10 AVAILABILITY/LIMITATION NOTICES		
NONE		
11 SUPPLEMENTARY NOTES		12. SPONSORING MILITARY ACTIVITY
		Department of the Navy Bureau of Ships Washington, D.C.
13 ABSTRACT		
<p>This report, the second of a series on studies of the wake in the propeller plane of ship models, presents the results of analysis of the wake of twin-screw, military-type ship models using the IBM-7090 computer. The data presented are the interpolated longitudinal and tangential velocity distributions, their computed mean values, the harmonic contents of these velocity components, the maximum variations in the resultant inflow velocity, and the advance angles and their variations. Also included are the calculated volumetric wake velocities.</p>		

DD FORM 1 JAN 64 1473

UNCLASSIFIED  
Security Classification



Security Classification

14. KEY WORDS	LINK A		LINK B		LINK C	
	ROLE	WT	ROLE	WT	ROLE	WT
Wake Propeller Cavitation Vibration Naval Ships Digital Computer						

INSTRUCTIONS

1. **ORIGINATING ACTIVITY:** Enter the name and address of the contractor, subcontractor, grantee, Department of Defense activity or other organization (*corporate author*) issuing the report.
- 2a. **REPORT SECURITY CLASSIFICATION:** Enter the overall security classification of the report. Indicate whether "Restricted Data" is included. Marking is to be in accordance with appropriate security regulations.
- 2b. **GROUP:** Automatic downgrading is specified in DoD Directive 5200.10 and Armed Forces Industrial Manual. Enter the group number. Also, when applicable, show that optional markings have been used for Group 3 and Group 4 as authorized.
3. **REPORT TITLE:** Enter the complete report title in all capital letters. Titles in all cases should be unclassified. If a meaningful title cannot be selected without classification, show title classification in all capitals in parenthesis immediately following the title.
4. **DESCRIPTIVE NOTES:** If appropriate, enter the type of report, e.g., interim, progress, summary, annual, or final. Give the inclusive dates when a specific reporting period is covered.
5. **AUTHOR(S):** Enter the name(s) of author(s) as shown on or in the report. Enter last name, first name, middle initial. If military, show rank and branch of service. The name of the principal author is an absolute minimum requirement.
6. **REPORT DATE:** Enter the date of the report as day, month, year, or month, year. If more than one date appears on the report, use date of publication.
- 7a. **TOTAL NUMBER OF PAGES:** The total page count should follow normal pagination procedures, i.e., enter the number of pages containing information.
- 7b. **NUMBER OF REFERENCES:** Enter the total number of references cited in the report.
- 8a. **CONTRACT OR GRANT NUMBER:** If appropriate, enter the applicable number of the contract or grant under which the report was written.
- 8b, 8c, & 8d. **PROJECT NUMBER:** Enter the appropriate military department identification, such as project number, subproject number, system numbers, task number, etc.
- 9a. **ORIGINATOR'S REPORT NUMBER(S):** Enter the official report number by which the document will be identified and controlled by the originating activity. This number must be unique to this report.
- 9b. **OTHER REPORT NUMBER(S):** If the report has been assigned any other report numbers (*either by the originator or by the sponsor*), also enter this number(s).
10. **AVAILABILITY/LIMITATION NOTICES:** Enter any limitations on further dissemination of the report, other than those

imposed by security classification, using standard statements such as:

- (1) "Qualified requesters may obtain copies of this report from DDC."
- (2) "Foreign announcement and dissemination of this report by DDC is not authorized."
- (3) "U. S. Government agencies may obtain copies of this report directly from DDC. Other qualified DDC users shall request through \_\_\_\_\_."
- (4) "U. S. military agencies may obtain copies of this report directly from DDC. Other qualified users shall request through \_\_\_\_\_."
- (5) "All distribution of this report is controlled. Qualified DDC users shall request through \_\_\_\_\_."

If the report has been furnished to the Office of Technical Services, Department of Commerce, for sale to the public, indicate this fact and enter the price, if known.

11. **SUPPLEMENTARY NOTES:** Use for additional explanatory notes.
12. **SPONSORING MILITARY ACTIVITY:** Enter the name of the departmental project office or laboratory sponsoring (*paying for*) the research and development. Include address.
13. **ABSTRACT:** Enter an abstract giving a brief and factual summary of the document indicative of the report, even though it may also appear elsewhere in the body of the technical report. If additional space is required, a continuation sheet shall be attached.

It is highly desirable that the abstract of classified reports be unclassified. Each paragraph of the abstract shall end with an indication of the military security classification of the information in the paragraph, represented as (TS), (S), (C), or (U).

There is no limitation on the length of the abstract. However, the suggested length is from 150 to 225 words.

14. **KEY WORDS:** Key words are technically meaningful terms or short phrases that characterize a report and may be used as index entries for cataloging the report. Key words must be selected so that no security classification is required. Identifiers, such as equipment model designation, trade name, military project code name, geographic location, may be used as key words but will be followed by an indication of technical content. The assignment of links, rules, and weights is optional.